Soil nutrient competitive traits of plants, microbes, and mineral surfaces explain nutrient acquisition in tropical experimental manipulations

Qing Zhu[1*], William J. Riley[1], Jinyun Tang[1], Charles D. Koven[1]

[1] Climate Sciences Department, Earth Sciences Division, Lawrence Berkeley National Laboratory, Berkeley, CA 94720

[*] Correspondence to: Q. Zhu (qzhu@lbl.gov)

Abstract

Soil is a complex system where biotic (*e.g.*, plant roots, micro-organisms) and abiotic (*e.g.*, mineral surfaces) consumers compete for resources necessary for life (*e.g.*, nitrogen, phosphorus). This competition is ecologically significant, since it regulates the dynamics of soil nutrients and controls aboveground plant productivity. Here we develop, calibrate, and test a nutrient competition model that accounts for multiple soil nutrients interacting with multiple biotic and abiotic consumers. As applied here for tropical forests, the Nutrient COMpetition model (N-COM) includes three primary soil nutrients (NH_4^+, NO_3^-, and PO_x (representing the sum of PO_4^{3-}, HPO_4^{2-}, and $H_2PO_4^-$)) and five potential competitors (plant roots, decomposing microbes, nitrifiers, denitrifiers, and mineral surfaces). The competition is formulated with a quasi-steady-state chemical equilibrium approximation to account for substrate (multiple substrates share one consumer) and consumer (multiple consumers compete for one substrate) effects. N-COM successfully reproduced observed soil heterotrophic respiration, N_2O emissions, free phosphorus, sorbed phosphorus, and NH_4^+ pools at a tropical forest site (Tapajos). The overall model posterior uncertainty was moderately well constrained. Our sensitivity analysis revealed that soil nutrient competition was primarily regulated by consumer-

substrate affinity rather than environmental factors such as soil temperature or soil moisture. Our results also imply that under strong nutrient limitation, relative competitiveness depends strongly on the competitor functional traits (affinity and nutrient carrier enzyme abundance). We then applied the N-COM model to analyze field nitrogen and phosphorus perturbation experiments in two tropical forest sites (in Hawaii and Puerto Rico) not used in model development or calibration. Under soil inorganic nitrogen and phosphorus elevated conditions, the model accurately replicated the experimentally observed competition among nutrient consumers. Although we used as many observations as we could obtain, more nutrient addition experiments in tropical systems would greatly benefit model testing and calibration. In summary, the N-COM model provides an ecologically consistent representation of nutrient competition appropriate for land BGC models integrated in Earth System Models.

1 Introduction

Atmospheric CO_2 concentrations have risen sharply since the pre-industrial era, primarily due to anthropogenic fossil fuel combustion and land use and land cover change [*Houghton*, 2003; *Le Quéré et al.*, 2013; *Marland et al.*, 2003]. Terrestrial ecosystems mitigate the increasing atmospheric CO_2 trend by absorbing roughly a quarter of anthropogenic CO_2 emissions [*Le Quéré et al.*, 2009]. However, it is still an open question whether the terrestrial CO_2 sink can be sustained [*Sokolov et al.*, 2008; *Zaehle et al.*, 2010], given that plant productivity is generally limited by soil nutrients [*Elser et al.*, 2007; *LeBauer and Treseder*, 2008; *Vitousek and Howarth*, 1991] and soil nutrients could be quickly depleted through biogeochemical [*Chauhan et al.*, 1981; *Nordin et al.*, 2001; *Shen et al.*, 2011] and hydrological [*Dise and Wright*, 1995; *Perakis and Hedin*, 2002] processes. Therefore, a holistic representation of soil nutrient dynamics is critically important to model the responses of terrestrial ecosystem CO_2 uptake to climate change.

Until recently, land models integrated in Earth System Models (ESMs) have largely ignored the close coupling between soil nutrient dynamics and the carbon cycle, although the impacts of soil nutrients (primarily Nitrogen and Phosphorus) regulating carbon-climate feedback are clearly required in ecosystem biogeochemistry and land models [*Zaehle and Dalmonech*, 2011; *Zhang et al.*, 2011]. For example, none of the land models in C^4MIP (Coupled Climate Carbon Cycle Model Intercomparison Project phase 4) had coupled Carbon and Nitrogen dynamics [*Friedlingstein et al.*, 2006]. The current generation of CMIP5 [*Anav et al.*, 2013] models used for the recent IPCC (Intergovernmental Panel on Climate Change) assessment had only two members (CLM4CN: *Thornton et al.* [2007]; and BNU-ESM: [*Ji et al.*, 2014]) that considered

59 nitrogen regulation of terrestrial carbon dynamics. However, as discussed below, several
60 recent studies have shown that these models had large biases in most of the individual
61 processes important for simulating nutrient dynamics. We therefore believe that, at the
62 global scale, no credible representation of nutrient constraints on terrestrial carbon
63 cycling yet exists in ESMs.

64 Further, none of the CMIP5 ESMs included a phosphorus cycle, which is likely
65 important for tropical forest carbon budgets [*Vitousek and Sanford*, 1986]. The recent
66 IPCC report highlights the importance of nitrogen and phosphorus availability on land
67 carbon storage, even though the phosphorus limitation effect is uncertain [*Stocker et al.*,
68 2013]. Since the next generation of ESMs participating in the CMIP6 synthesis will
69 continue to focus on the impacts of a changing climate on terrestrial CO_2 and abiotic
70 exchanges with the atmosphere [*Provides*, 2014], developing ecologically realistic and
71 observationally-constrained representations of soil nutrient dynamics and carbon-nutrient
72 interactions in ESMs is critical.

73 The importance of nutrient limitations in terrestrial ecosystems has been widely
74 demonstrated by nitrogen and phosphorus fertilization experiments [*Elser et al.*, 2007].
75 For instance, plant Net Primary Production (NPP) is enhanced in plots with nutrient
76 addition [*LeBauer and Treseder*, 2008]. Similarly, plant growth can be stimulated due to
77 atmospheric nitrogen deposition [*Matson et al.*, 2002]. Boreal forests are strongly limited
78 by nitrogen availability [*Vitousek and Howarth*, 1991], because low temperatures reduce
79 nitrogen mineralization [*Bonan and Cleve*, 1992] and N_2 fixation [*DeLuca et al.*, 2008;
80 *DeLuca et al.*, 2002]. In contrast, tropical forests are often phosphorus limited [*Vitousek*
81 *et al.*, 2010], since tropical soils are old and phosphorus derived from parent material

82 weathering has been depleted through long-term pedogenesis processes [*Vitousek and*
83 *Farrington*, 1997; *Walker and Syers*, 1976]. In natural ecosystems without external
84 nutrients inputs (*e.g.*, N deposition), soil nitrogen or phosphorus (or both) are likely
85 insufficient to satisfy both plant and microorganism demands [*Vitousek and Farrington*,
86 1997]. Plants have to compete with microorganisms and mineral surfaces [*Kaye and*
87 *Hart*, 1997; *Schimel et al.*, 1989] to obtain sufficient nutrients to sustain their biological
88 processes (*e.g.*, photosynthesis, respiration). Therefore, it is critical to improve the
89 representation of nutrient competition to accurately model how terrestrial ecosystems will
90 respond to perturbations in soil nutrient dynamics (*e.g.*, from elevated nitrogen deposition
91 or CO_2 fertilization-induced nutrient requirements).
92 Intense competition between plants and microorganisms is a well-observed
93 phenomenon in nutrient-limited systems [*Hodge et al.*, 2000a; *Johnson*, 1992; *Kaye and*
94 *Hart*, 1997]. Previously, plants were thought to be initial losers in nutrient competition,
95 due to the fact that microbes are more intimately associated with substrates [*Woodmansee*
96 *et al.*, 1981]. However, increasing observational evidence indicates that plants compete
97 effectively with soil microorganisms [*Schimel and Bennett*, 2004] under certain
98 circumstances; sometime even outcompeting them and suppressing microbial growth [*Hu*
99 *et al.*, 2001; *J Wang and Lars*, 1997]. ^{15}N isotope studies have also demonstrated that
100 plants can capture a large fraction of added nitrogen [*Hodge et al.*, 2000b; *Marion et al.*,
101 1982]. In the short term (days to months), plants maintain their competitiveness mainly
102 through (1) establishing mycorrhizal fungi associations [*Drake et al.*, 2011; *Rillig et al.*,
103 1998], which help plants acquire organic and inorganic forms of nitrogen [*Hobbie and*
104 *Hobbie*, 2006; *Hodge and Fitter*, 2010] and (2) root exudation of extracellular enzymes

105 that decompose rhizosphere soil organic matter [*Phillips et al.*, 2011]. In the relatively
106 longer term (months to years), morphological adjustment occurs; for example, plants
107 allocate more carbon to fine roots to explore laterally and deeper [*Iversen et al.*, 2011;
108 *Jackson et al.*, 2009]. Finally, over the course of years to decades, plant succession can
109 occur [*Medvigy et al.*, 2009; *Moorcroft et al.*, 2001] and the new plant demography will
110 need to be considered to represent nutrient controls on this time scale.
111 Given these patterns from the observational literature, nutrient competition is
112 either absent or over-simplified in existing Earth System Models (ESMs). One common
113 representation of plant-microbe competition is that plants compete poorly against
114 microbes in resource acquisition. For example, the O-CN land model [*Zaehle and Friend*,
115 2010] assumes that soil decomposing microbes have the priority to immobilize soil
116 mineral nitrogen. After microbes meet their demands, the remaining nitrogen is then
117 available for plant uptake.
118 Another treatment in ESM land models is that microbial and plant nutrient
119 acquisition competitiveness is based on their relative demands. For example, CLM4CN
120 [*Thornton et al.*, 2007] assumes that the plant and microbial nitrogen demands are
121 satisfied simultaneously. Under nitrogen infertile conditions, all nitrogen demands in the
122 system are down-regulated proportional to the individual demands and subject to
123 available soil mineral nitrogen. This approach led to unrealistic diurnal cycles of gross
124 primary production (GPP), with midday depressions in GPP occurring because of
125 predicted diurnal depletion of the soil mineral nitrogen pool. Emergent impacts of this
126 conceptualization of nutrient constraints on GPP resulted in poor predictions compared to
127 observations, with smaller than observed plant C growth responses to N deposition

[*Thomas et al.*, 2013a] and larger than observed responses to N fertilization [*Thomas et al.*, 2013b]. Further, most biogeochemistry models not integrated in ESMs also adopt one of these approaches. For instance, Biome-BGC [*Running and Coughlan*, 1988], CENTURY [*Parton et al.*, 1988], CASA (Carnegie-Ames-Stanford Approach; [*Potter et al.*, 1993]) and the Terrestrial Ecosystem Model - TEM [*McGuire et al.*, 1992] assume that available nutrients preferentially satisfy the soil microbial immobilization demand.

We believe the two conceptualizations of competition used in ESMs substantially over-simplify competitive interactions between plants and microbes and lead to biases in carbon cycle predictions. To begin to address the problems with these simplified approaches, Tang and Riley (2013) showed that complex consumer-substrate networks can be represented with an approach (called Equilibrium Chemical Approximation (ECA) kinetics) that simultaneously resolves multiple demands for multiple substrates, and demonstrated that the approach was consistent with observed litter decomposition observations. ECA kinetics has also recently been applied to analyze the emergent temperature response of SOM decomposition, considering equilibrium, non-equilibrium, and enzyme temperature sensitivities and abiotic interactions with mineral surfaces [*Tang and Riley*, 2014]. We extend on that work here by presenting an implementation of ECA kinetics to represent competition for multiple soil nutrients in a multiple consumer environment. We note that this paper demonstrates a method to handle instantaneous competition in the complex soil-plant network, but a robust competition representation for climate-scale models will require representation of dynamic changes in plant allocation and plant composition.

The aim of this study is to provide a reliable nutrient competition approach applicable for land models integrated in ESMs. However, before integration into an ESM, the competition model needs to be carefully calibrated and independently tested against observational data. This paper will therefore focus on model development and evaluation at several tropical forest sites where observations are available. Our objectives are to: (1) develop a soil biogeochemistry model with multiple nutrients (*i.e.*, NH_4^+, NO_3^-, and PO_x (represented as the sum of PO_4^{3-}, HPO_4^{2-}, and $H_2PO_4^-$)) and multiple nutrient consumers (*i.e.*, decomposing microbes, plants, nitrifiers, denitrifiers, and mineral surfaces) competition using ECA kinetics [*Tang and Riley*, 2013; *Zhu and Riley*, 2015]; (2) constrain the model with *in situ* observational datasets of soil carbon, nitrogen, and phosphorus dynamics using a Markov Chain Monte Carlo (MCMC) approach; and (3) test model performance against nitrogen and phosphorus fertilization studies.

2 Method

2.1 Model development

The Nutrient COMpetition model (N-COM) is designed as a soil biogeochemistry model (Figure 1) to simulate soil carbon decomposition, nitrogen and phosphorus transformations, abiotic interactions, and plant demands. Although our ultimate goal is to incorporate N-COM into a decomposition model that represents active microbial activity as the primary driver of decomposition, we start here by presenting the N-COM approach using a Century-like [*Koven et al.*, 2013; *Parton et al.*, 1988] structure, with additions to account for phosphorus dynamics. In our approach, we calculate potential immobilization using literature-derived parameters (*e.g.*, *VMAX*, *KM*) in a Michaelis-Menten (MM) kinetics framework. The potential immobilization is subsequently modified using the ECA competition method.

Five pools of soil organic Carbon (C), Nitrogen (N), and Phosphorus (P) are considered: Coarse Wood Debris (CWD), litter, fast Soil Organic Matter (SOM) pool, medium SOM pool, and slow SOM pool. Litter is further divided into three sub-groups: metabolic, cellulose, and lignin. The soil organic C, N, and P decomposition ($F_{C,j}^{dec}$, $F_{N,j}^{dec}$, $F_{P,j}^{dec}$) follow first-order decay:

$$F_{C,j}^{dec} = k_j C_j r_\theta r_T \quad (1)$$

$$F_{N,j}^{dec} = k_j N_j r_\theta r_T \quad (2)$$

$$F_{P,j}^{dec} = k_j P_j r_\theta r_T \quad (3)$$

where k_j is the rate constant of soil organic matter decay (s^{-1}); C_j, N_j, and P_j are pool sizes (g m^{-2}) of carbon, nitrogen, and phosphorus, respectively (*j* from 1 to 7 represents the soil organic matter pools: CWD, metabolic litter, cellulose litter, lignin litter, fast

SOC, median SOC, slow SOC); r_T and r_θ (dimensionless) are soil temperature and moisture environmental regulators.

Decomposed carbon ($F_{C,i}^{dec}$) (upstream i^{th} pool) either (1) enters a downstream pool (j^{th}) or (2) is lost as CO_2. Soil organic carbon (downstream j^{th} pool) temporal change is calculated as:

$$\frac{dC_j}{dt} = -F_{C,j}^{dec} + \sum_{i=1}^{N} F_{C,ij}^{move} \quad (4)$$

where $\sum_{i=1}^{N} F_{C,ij}^{move}$ is the summation of carbon fluxes that move from the upstream pool (i) to the downstream pool (j) due to the decomposition of upstream SOC. For each upstream carbon pool (i = *1, 2, ..., 7*), the fractions integrated into downstream pools (j = *1, 2, ..., 7*) is summarized in a 7×7 matrix f_{ij} (Table 2). The percentage of decomposed carbon that is respired as CO_2 is represented by g_i (Table 2). Simultaneously, soil organic N and P changes follow C decomposition:

$$\frac{dN_j}{dt} = -F_{N,j}^{dec} + \sum_{i=1}^{N} F_{N,ij}^{move} + \sum_{i=1}^{N} F_{NH4,ij}^{immob} + \sum_{i=1}^{N} F_{NO3,ij}^{immob} \quad (5)$$

$$\frac{dP_j}{dt} = -F_{P,j}^{dec} + \sum_{i=1}^{N} F_{P,ij}^{move} + \sum_{i=1}^{N} F_{P,ij}^{immob} \quad (6)$$

where $F_{N,ij}^{move}$ and $F_{P,ij}^{move}$ are fluxes of nitrogen and phosphorus moving from the upstream (i) to downstream (j) pools. $F_{NH4,ij}^{immob}$, $F_{NO3,ij}^{immob}$, and $F_{P.ij}^{immob}$ are immobilization fluxes of soil mineral nitrogen and phosphorus. $F_{N,j}^{dec}$ and $F_{P,j}^{dec}$ represent soil organic matter decomposition losses.

Equations (5) and (6) state that changes in the j^{th} organic N or P pool are the summation of three terms: (1) organic N and P lost during soil organic matter mineralization ($-F_{N,j}^{dec}$ and $-F_{P,j}^{dec}$); (2) a fraction of the i^{th} organic N or P pool (upstream) enters into the j^{th} pool (downstream) ($F_{N,ij}^{move}$ and $F_{P,ij}^{move}$); and (3) soil microbial immobilization ($F_{NH4,ij}^{immob}$, $F_{NO3,ij}^{immob}$, and $F_{P,ij}^{immob}$). Immobilization occurs only when the newly entering organic N is insufficient to sustain the soil C:N (or C:P) ratio (more details described in Appendix A).

The inorganic nitrogen pools (NH_4^+ and NO_3^- (Eqn. 7 -8)) are altered by production (organic N mobilized by microbes), consumption (uptake by plants and microbes, gaseous or aqueous losses), and transformation (nitrification and denitrification). Inorganic P (PO_x) is assumed to be either taken up by plants and decomposing microbes or adsorbed to mineral surfaces (Eqn. 9). Plants utilize all forms of phosphate (*e.g.*, PO_4^{3-}, HPO_4^{2-}, and $H_2PO_4^-$), but for simplicity we use the symbol PO_x to represent the sum of all possible phosphate forms throughout the paper.

$$\frac{d[NH4]}{dt} = \sum_{j=1}^{N}\sum_{i=1}^{N} F_{NH4,ij}^{mob} - F_{NH4}^{nit} - F_{NH4}^{plant} - F_{NH4}^{immob} + F^{BNF} + F_{NH4}^{dep} \quad (7)$$

$$\frac{d[NO3]}{dt} = -F_{NO3}^{den} + (1 - f^{N2O})F_{NH4}^{nit} - F_{NO3}^{plant} - F_{NO3}^{immob} - F_{NO3}^{leach} + F_{NO3}^{dep} \quad (8)$$

$$\frac{d[PO_x]}{dt} = \sum_{j=1}^{N}\sum_{i=1}^{N} F_{P,ij}^{mob} - F_P^{plant} - F_P^{immob} - F_P^{surf} - F_P^{leach} + F^{weather} \quad (9)$$

where $F_{NH4,ij}^{mob}$ and $F_{P,ij}^{mob}$ are gross mineralization rates for nitrogen and phosphorus. F_{NH4}^{nit} is the nitrification flux, part of which is lost through a gaseous pathway (f^{N2O}) and the rest is incorporated into the NO_3^- pool. F_{NO3}^{den} is the denitrification flux, which transforms nitrate to N_2O and N_2 which then leave the soil system. Plant uptake of soil NH_4^+, NO_3^-,

and PO_x are represented as F_{NH4}^{plant}, F_{NO3}^{plant}, and F_P^{plant}, respectively. Soil decomposing microbial immobilization of soil NH_4^+, NO_3^-, and PO_x are represented as F_{NH4}^{immob}, F_{NO3}^{immob}, and F_P^{immob}. F_{NO3}^{leach}, and F_P^{leach} are leaching losses of soil NO_3^- and PO_x. External inputs into soil inorganic N pools include atmospheric ammonia deposition (F_{NH4}^{dep}), atmospheric nitrate deposition (F_{NO3}^{dep}), and biological nitrogen fixation (F^{BNF}). External sources of phosphate come from parent material weathering ($F^{weather}$).

Finally, the dynamics of sorbed P (P_S), occluded P (P_O), and parent material P (P_P) are modeled as:

$$\frac{d[P_S]}{dt} = F_P^{surf} - F_P^{occl} \quad (10)$$

$$\frac{d[P_O]}{dt} = F_P^{occl} \quad (11)$$

$$\frac{d[P_P]}{dt} = -F^{weather} + F_P^{dep} \quad (12)$$

where the pool of sorbed P is balanced by the adsorption flux (F_P^{surf}) and occlusion flux (F_P^{occl}). Parent material is lost by weathering ($F^{weather}$) and is slowly replenished by external atmospheric phosphorus inputs (F_P^{dep}, such as dust). More detailed information on the modeled C, N, and P fluxes is documented in Appendix A.

2.2 Multiple-consumer-multiple-resource competition network

The soil biogeochemistry model presented in **section 2.1** has multiple potential nutrient consumers (plants, SOM decomposing microbes, nitrifiers, denitrifiers, mineral surfaces) and multiple soil nutrients (NH_4^+, NO_3^-, PO_x). The consumer-resource network is summarized in Table 1. As in many land BGC models (CLM, Century, *etc.*), we have

not explicitly included the mineral surface adsorptions of NH_4^+ and NO_3^-, since we assume ammonia is quickly protected by mineral surfaces from leaching (no leaching term in Eqn. 7) but then released for plant and microbial uptake when the biotic demand arises. An improved treatment of these dynamics would necessitate a prognostic model for pH, which is beyond the scope of this analysis. Unlike sorbed P (which can be occluded), there is no further abiotic loss of sorbed ammonia. Therefore, the free ammonia pool is interpreted in the current model structure as a potential free ammonia pool (free + sorbed).

Competition between different consumers in acquiring different resources is summarized in Table 1. Each consumer-substrate competition reaction is represented by:

$$S + E \underset{k_1^-}{\overset{k_1^+}{\rightleftharpoons}} C \xrightarrow{k_2^+} P + E \tag{13}$$

The enzyme (*E: e.g., nutrient carrier enzyme produced by plants and microbes*) and substrate (*S: e.g., NH_4^+, NO_3^-*) reaction (reversible reaction) forms a substrate-enzyme complex (*C*). The following irreversible reaction leads to product (*P: meaning the nutrients has been taken up*) and releases enzyme (*E*) back into soil media. For the whole complex reaction network, nutrient uptakes are formulated as:

$$F_{NH4}^{plant} = k_{NH4}^{plant} \cdot \frac{[NH4] \cdot [E_N^{plant}]}{KM_{NH4}^{plant}(1 + \frac{[NH4]}{KM_{NH4}^{plant}}^{(1)} + \frac{[NO3]}{KM_{NO3}^{plant}}^{(2)} + \frac{[E_N^{plant}]}{KM_{NH4}^{plant}}^{(3)} + \frac{[E_N^{mic}]}{KM_{NH4}^{mic}}^{(4)} + \frac{[E_N^{nit}]}{KM_{NH4}^{nit}}^{(5)})} \tag{14}$$

$$F_{NH4}^{immob} = k_{NH4}^{immob} \cdot \frac{[NH4] \cdot [E_N^{mic}]}{KM_{NH4}^{mic}(1 + \frac{[NH4]}{KM_{NH4}^{mic}} + \frac{[NO3]}{KM_{NO3}^{mic}} + \frac{[E_N^{plant}]}{KM_{NH4}^{plant}} + \frac{[E_N^{mic}]}{KM_{NH4}^{mic}} + \frac{[E_N^{nit}]}{KM_{NH4}^{nit}})} \tag{15}$$

$$F_{NH4}^{nit} = k_{NH4}^{nit} \cdot \frac{[NH4] \cdot [E_{NH4}^{nit}]}{KM_{NH4}^{nit}(1 + \frac{[NH4]}{KM_{NH4}^{nit}} + \frac{[E_N^{plant}]}{KM_{NH4}^{plant}} + \frac{[E_N^{mic}]}{KM_{NH4}^{mic}} + \frac{[E_N^{nit}]}{KM_{NH4}^{nit}})} \tag{16}$$

$$F_{NO3}^{plant} = k_{NO3}^{plant} \cdot \frac{[NO3] \cdot [E_N^{plant}]}{KM_{NO3}^{plant}(1 + \frac{[NH4]}{KM_{NH4}^{plant}} + \frac{[NO3]}{KM_{NO3}^{plant}} + \frac{[E_N^{plant}]}{KM_{NO3}^{plant}} + \frac{[E_N^{mic}]}{KM_{NO3}^{mic}} + \frac{[E_N^{den}]}{KM_{NO3}^{den}})} \quad (17)$$

$$F_{NO3}^{immob} = k_{NO3}^{immob} \cdot \frac{[NO3] \cdot [E_N^{mic}]}{KM_{NO3}^{mic}(1 + \frac{[NH4]}{KM_{NH4}^{mic}} + \frac{[NO3]}{KM_{NO3}^{mic}} + \frac{[E_N^{plant}]}{KM_{NO3}^{plant}} + \frac{[E_N^{mic}]}{KM_{NO3}^{mic}} + \frac{[E_N^{den}]}{KM_{NO3}^{den}})} \quad (18)$$

$$F_{NO3}^{den} = k_{NO3}^{den} \cdot \frac{[NO3] \cdot [E_{NO3}^{den}]}{KM_{NL3}^{den}(1 + \frac{[NO3]}{KM_{NO3}^{den}} + \frac{[E_N^{plant}]}{KM_{NO3}^{plant}} + \frac{[E_N^{mic}]}{KM_{NO3}^{mic}} + \frac{[E_N^{den}]}{KM_{NO3}^{den}})} \quad (19)$$

$$F_P^{plant} = k_P^{plant} \cdot \frac{[PO_x] \cdot [E_P^{plant}]}{KM_P^{plant}(1 + \frac{[PO_x]}{KM_P^{plant}} + \frac{[E_P^{plant}]}{KM_P^{plant}} + \frac{[E_P^{mic}]}{KM_P^{mic}} + \frac{[E_P^{surf}]}{KM_P^{surf}})} \quad (20)$$

$$F_P^{mic} = k_P^{mic} \cdot \frac{[PO_x] \cdot [E_P^{mic}]}{KM_P^{mic}(1 + \frac{[PO_x]}{KM_P^{mic}} + \frac{[E_P^{plant}]}{KM_P^{plant}} + \frac{[E_P^{mic}]}{KM_P^{mic}} + \frac{[E_P^{surf}]}{KM_P^{surf}})} \quad (21)$$

$$F_P^{surf} = k_P^{surf} \cdot \frac{[PO_x] \cdot [E_P^{mic}]}{KM_P^{surf}(1 + \frac{[PO_x]}{KM_P^{surf}} + \frac{[E_P^{plant}]}{KM_P^{plant}} + \frac{[E_P^{mic}]}{KM_P^{mic}} + \frac{[E_P^{surf}]}{KM_P^{surf}})} \quad (22)$$

where F represent the nutrient uptake fluxes and k is the base reaction rate that enzyme-substrate complex forms product (k_2^+ in Eqn. 13). [E] and KM denote enzyme abundance and half saturation constants (substrate-enzyme affinity). Superscripts and subscripts refer to consumers and substrates, respectively. These equations account for the effect of (1) multiple substrates (*e.g.*, NH_4^+ and NO_3^-) sharing one consumer, which inhibits the effective binding between any specific substrate and the consumer (terms $^{(1)}$ and $^{(2)}$ in Eqn. 14) and (2) multiple consumers (*e.g.*, plants, decomposing microbes, and nitrifiers)

sharing one substrate (*e.g.*, NH_4^+), which lowers the probability of effective binding between any consumer and NH_4^+ (terms $^{(3)}$, $^{(4)}$, and $^{(5)}$ in Eqn. 14).

For our reaction network (Eqn. 13 – 22), we assume that: (1) plant roots and decomposing microbes possess two types of nutrient carrier enzymes (nutrient transporters). One is for nitrogen (NH_4^+ and NO_3^-; E_N^{plant}, E_N^{mic}), and the other is for phosphorus, including different forms of phosphate (E_P^{plant}, E_P^{mic}). (2) Nutrient carrier enzyme abundance is scaled with biomass (fine root or microbial biomass). Scaling factors are 0.0000125 (for plants) and 0.05 (for decomposing microbes) (Table 2). (3) Mineral surface "effective enzyme" abundance (E_P^{surf}) is approximated by the available sorption surface area ($VMAX_P^{surf} - [SP]$). (4) Nitrifiers and denitrifiers are not explicitly simulated, therefore we assume that their biomass and associated nutrient transporter abundance are fixed (E_N^{nit}, E_N^{denit}).

For simplicity, we group the "decomposing microbes/nitrifier/denitrifier/mineral surface nutrient carrier enzyme [*E*]" and their "base reaction rate *k*" into one single variable "*VMAX*" (see Appendix B for full derivation). Furthermore, we defined "potential rates (potential immoblizaiton, nitrification, denitrification, adsorption rates)" and used them as proxies of "*VMAX*". Therefore, Eqn. 15, 16, 18, 19, 21, 22 become:

$$F_{NH4}^{immob} = F_{NH4}^{immob,pot} \cdot \frac{[NH4]}{KM_{NH4}^{mic}(1+\frac{[NH4]}{KM_{NH4}^{mic}}+\frac{[NO3]}{KM_{NO3}^{mic}}+\frac{[E_N^{plant}]}{KM_{NH4}^{plant}}+\frac{[E_N^{mic}]}{KM_{NH4}^{mic}}+\frac{[E_N^{nit}]}{KM_{NH4}^{nit}})} \quad (23)$$

$$F_{NH4}^{nit} = F_{NH4}^{nit,pot} \cdot \frac{[NH4]}{KM_{NH4}^{nit}(1+\frac{[NH4]}{KM_{NH4}^{nit}}+\frac{[E_N^{plant}]}{KM_{NH4}^{plant}}+\frac{[E_N^{mic}]}{KM_{NH4}^{mic}}+\frac{[E_N^{nit}]}{KM_{NH4}^{nit}})} \quad (24)$$

$$F_{NO3}^{immob} = F_{NO3}^{immob,pot} \cdot \frac{[NO3]}{KM_{NO3}^{mic}(1+\frac{[NH4]}{KM_{NH4}^{mic}}+\frac{[NO3]}{KM_{NO3}^{mic}}+\frac{[E_N^{plant}]}{KM_{NO3}^{plant}}+\frac{[E_N^{mic}]}{KM_{NO3}^{mic}}+\frac{[E_N^{den}]}{KM_{NO3}^{den}})} \quad (25)$$

$$F_{NO3}^{den} = F_{NO3}^{den,pot} \cdot \frac{[NO3]}{KM_{NL3}^{den}(1+\frac{[NO3]}{KM_{NO3}^{den}}+\frac{[E_N^{plant}]}{KM_{NO3}^{plant}}+\frac{[E_N^{mic}]}{KM_{NO3}^{mic}}+\frac{[E_N^{den}]}{KM_{NO3}^{den}})} \quad (26)$$

$$F_P^{mic} = F_P^{immob,pot} \cdot \frac{[PO_x]}{KM_P^{mic}(1+\frac{[PO_x]}{KM_P^{mic}}+\frac{[E_P^{plant}]}{KM_P^{plant}}+\frac{[E_P^{mic}]}{KM_P^{mic}}+\frac{[E_P^{surf}]}{KM_P^{surf}})} \quad (27)$$

$$F_P^{surf} = F_P^{surf,pot} \cdot \frac{[PO_x]}{KM_P^{surf}(1+\frac{[PO_x]}{KM_P^{surf}}+\frac{[E_P^{plant}]}{KM_P^{plant}}+\frac{[E_P^{mic}]}{KM_P^{mic}}+\frac{[E_P^{surf}]}{KM_P^{surf}})} \quad (28)$$

In this case, the potential rates are treated as maximum reaction rates (*VMAX*), because they are calculated without nutrient constraints or biotic and abiotic interactions. For example, potential P immobilization rate ($F_P^{immob,pot}$) is based on the total phosphorus demand that can perfectly maintain the soil CP stoichiometry during soil organic matter decomposition (Eqn. A9). This potential immobilization rate represents the maximum phosphorus influx that the soil could take up at that moment. The maximum adsorption rate ($F_P^{surf,pot}$) is the time derivative of the Langmuir equation (Eqn. A12), which is a theoretically maximal adsorption rate excluding all other biotic and abiotic interactions. The potential rates (*VMAX*) are updated by the model rather than calibrated, except for $VMAX_P^{surf}$. $VMAX_P^{surf}$ denotes the maximum adsorption capacity (not maximum adsorption rate), which affects the potential adsorption rate ($F_P^{surf,pot}$).

The model is run on an hourly time step, initialized with state variables and critical parameters (Table 2). Since the model is designed to be a component of the

312 Community and ACME Land Models (CLM, ALM; which are essentially currently
313 equivalent), we used CLM4.5 site-level simulations to acquire temporally-resolved: (1)
314 soil temperature factors on decomposition (r_T); (2) soil moisture factors on
315 decomposition (r_θ); (3) the anoxic fraction of soil pores (f^{anox} in Appendix Eqn. A10-
316 11); (4) annual NPP (NPP_{annual} in Appendix Eqn. A13); (5) NH_4^+ deposition (F_{NH4}^{dep}); (6)
317 NO_3^- deposition (F_{NO3}^{dep}); and (7) hydrologic discharge (Q_{dis} in Appendix Eqn. A14).
318 External inputs of mineral phosphorus are derived from Mahowald *et al.*, [2005, 2008].

319 **2.3 Model parameterization and sensitivity analysis**

320 We constrained model parameters and performed sensitivity analyses using a suite
321 of observations distinct from the observations we used subsequently to test the model
322 against the N and P manipulation experiments. Because tropical systems can be either
323 nitrogen or phosphorous limited (or both) [*Elser et al.*, 2007; *Vitousek et al.*, 2010], we
324 chose observations from a tropical forest site to constrain the N and P competition in our
325 model (Tapajos National Forest, Para, Brazil (Table 3)).

326 In the parameter estimation procedure, several data streams are assimilated into
327 the N-COM model, including measurements of soil NH_4^+ concentrations, soil free
328 phosphate concentrations, sorbed phosphate concentrations, and N_2O and CO_2 flux
329 measurements. The datasets are summarized in Table 3 and cover a wide range of N and
330 P biogeochemistry dynamics. A set of model parameters is selected for calibration (Table
331 4), which comprise nutrient competition kinetics parameters (*k* and *KM*) as well as the
332 fast soil carbon turnover time ($TURN_{SOM}$). Because we had only a short-term CO_2
333 respiration flux record, we were unable to calibrate the longer turnover time parameters.
334 However, since we test the posterior model against short-term fertilization responses, this

335 omission will not affect our evaluation. Longer records from eddy covariance flux towers
336 and ^{14}C soil measurements are required to constrain the longer turnover time pool values.
337 We employed the Markov Chain Monte Carlo (MCMC) approach [*Ricciuto et al.*,
338 2008] to assimilate the observations into N-COM. MCMC directly draws samples from a
339 pre-defined parameter space and tries to minimize a pre-defined cost function:

340 $$J = (M(\theta) - D)^T R^{-1} (M(\theta) - D) \quad (29)$$

341 where $\boldsymbol{M(\theta)}$ and $\boldsymbol{D}$ are vectors of model outputs and observations including time series of
342 different simulated variables (*e.g.*, soil CO_2 and N_2O effluxes and soil concentrations of
343 NH_4^+, free PO_x, and sorbed PO_x); $\boldsymbol{\theta}$ is a vector of model parameters ($\boldsymbol{\theta_i}$); and $\boldsymbol{i}$ from 1 to
344 20 represents the parameters that are calibrated (Table 4). R^{-1} is the inverse of data error
345 covariance matrix. We assumed that diagonal elements are 40% of observed values and
346 off-diagonal elements are zeros. We further assumed that the prior parameter follows a
347 lognormal distribution. μ and σ were 0.91 and 0.95 of their initial values, respectively
348 (Table 4). We then ran MCMC to sample 50,000 parameter pairs (Fig. A1). The second
349 half of the samples was used to calculate the posterior parameter space by fitting to a
350 Gaussian distribution. We also employed the Gelman-Rubin criterion to quantitatively
351 show whether or not the MCMC chain converged. The posterior model parameters are
352 reported in term of means and standard deviations. Uncertainty Reduction (*UR*) is
353 calculated based on (1) variance (Eqn. 30a) and (2) 25% and 75% quantile (Eqn. 30b):

354 $$UR_\sigma = (1 - \frac{\sigma_{posterior}}{\sigma_{prior}}) \cdot 100\% \quad (30a)$$

355 $$UR_Q = (1 - \frac{Q^{75}_{posterior} - Q^{25}_{posterior}}{Q^{75}_{prior} - Q^{25}_{prior}}) \cdot 100\% \quad (30b)$$

where σ_{prior} is prior parameter uncertainty, which is 95% of the parameter initial value. $\sigma_{posterior}$ is posterior parameter uncertainty, which is calculated by fitting the posterior model parameters to a Gaussian distribution. Q^{75} and Q^{25} are 75% and 25% percentage quantile of each parameter. Uncertainty Reduction is a useful metric [*Zhu and Zhuang*, 2014], because it quantitatively reveals the reduction in the range of a particular parameter after calibration with MCMC. It does not, however, indicate that the parameter itself is more consistent with observed values of the parameter. A large value of *UR* implies a more robust posterior model.

In addition, we conducted a sensitivity study to identify the dominant controlling factors regulating nutrient competition in N-COM. Three scenarios were considered: (1) baseline climate and soil conditions; (2) elevated soil temperature (by 5 °C); and (3) elevated soil moisture (by 50%). SOBOL sampling [*Pappas et al.*, 2013], a global sensitivity technique, is employed to calculate the sensitivities of output variables with respect to various inputs:

$$S_i = \frac{VAR_{p_i}(E_{p_{\sim i}}(Y \mid p_i))}{VAR(Y)} \tag{31}$$

where S_i is the first order sensitivity index of the i^{th} parameter and ranges from 0 to 1. By comparing the values of S_i, we were able to evaluate which processes were relatively more important in affecting nutrient competition. Y represents the model outputs of plant NH_4^+, NO_3^-, or PO_x uptake; p_i is the target parameter; $p_{\sim i}$ denotes all parameters that are associated with nutrient competition except the target parameter; and *VAR(.)* and *E(.)* represent variance and mean, respectively.

2.4 Model application

After calibration, we applied the N-COM model to several tropical forest nutrient fertilization studies not included in the calibration dataset, where isotopically labeled nitrogen or phosphorous fertilizer was injected into the soil. The fertilization experiments measured the fate of added nutrients; for example, identifying the fraction of added N or P that goes into the plant, is immobilized by microbes, or is stabilized by mineral surfaces. These measurements offer an effective baseline to test whether the N-COM model captures short-term nutrient competition.

Because we have focused in this paper on applications in tropical forests, we choose three tropical forest fertilization experiments with (1) PO_4^{3-}; (2) NH_4^+; and (3) NO_3^- additions (Table 5). The PO_4^{3-} fertilization experiment [*Olander and Vitousek*, 2005] was conducted in three Hawaiian tropical forests along a soil chronosequence (300, 20000, and 4100000 year old soils) that were fertilized with 10 μg g^{-1} $^{32}PO_4^{3-}$, respectively, and microbial demand versus soil sorption was measured. We did not evaluate the role of plants in phosphorus competition for the Hawaii sites, since plant phosphorus uptake was not measured in those field studies. Our model discriminates the Hawaii sites along the chronosequence by setting distinct initial pool sizes (derived from [*Olander and Vitousek*, 2004; *Olander and Vitousek*, 2005]) of soil organic carbon, nitrogen and phosphorus, and soil parent material phosphorus.

We also used measurements from NH_4^+ and NO_3^- fertilization studies located at the Luquillo tropical forest in Puerto Rico [*Templer et al.*, 2008]. In that study, 4.6 μg g^{-1} $^{15}NH_4^+$ was added into the highly weathered tropical forest soil and the consumption of $^{15}NH_4^+$ by plant roots, decomposing microbes, and nitrifiers were measured. In the same study, 0.92 μg g^{-1} $^{15}NO_3^-$ was added to the soil and the plant uptake and microbial

401 immobilization was measured. The measurements were made 24 or 48 hours after the
402 fertilizers were added.
403 For the model scenarios, we (1) spun up the N-COM model for 100 years; (2)
404 perturbed the soil nutrient pool by the same amount as the fertilization; (3) ran the model
405 for 24 or 48 hours and calculated how much of the added nutrients were absorbed by
406 plants, microbes, or mineral surfaces; and (4) compared our model simulations with the
407 observed data to assess model predictability. The 100-year spin up simulation aimed at
408 eliminating the effects of imposed initial inorganic pool sizes on fertilization
409 experiments, rather than accumulating soil organic matter in the system, since we
410 initialized the soil organic carbon pools from CLM4.5 steady state predictions.
411
412 **3. Results and discussion**
413 **3.1 Posterior model parameters**
414 Our best estimates (second half of the MCMC chain) of the selected model
415 parameters based on the observations at the Tapajos National Forest, Para, Brazil are
416 shown in Figure 2. We found that posterior parameter samples were not heavily tailed
417 and they generally follow Gaussian distributions (Figure A3). In order to quantitatively
418 compare the posterior parameter distributions with prior distributions, we fit parameter
419 samples to a Gaussian distribution and estimated its means and standard deviations
420 (Table 4).
421 Even though the posterior mean was improved, the uncertainty of the posterior
422 model may still be relatively large. In other words, a prognostic prediction based on these
423 posterior parameters could be relatively uncertain [*Scholze et al.*, 2007], due to large

uncertainty associated with the posterior parameters. Therefore, we calculated the variance-based Uncertainty Reduction (UR_σ) (Eqn. 30a) to evaluate model improvement in terms of posterior uncertainty. We found that parameters' uncertainties were reduced by 13%~98%. This calculation might either overestimate or underestimate the UR_σ, due to the fact that the posterior parameters did not strictly follow Gaussian distributions. But the actual UR_σ should not be far from our estimates, because the posterior samples were not widely spread across the potential parameter space (Figure 2). The least constrained parameter was k_{NO3}^{plant} (reaction rate of plant nitrogen carrier enzyme with NO_3^- substrate). Two other NO_3^- dynamics related parameters were also not well constrained: UR_σ of KM_{NO3}^{mic} (half-saturation constant for decomposing microbe NO_3^- immobilization) and KM_{NO3}^{den} (half-saturation constant for denitrifier NO_3^- consumption) were only 63% and 68%, respectively. Compared with NH_4^+ or PO_x competition related parameters, we concluded that parameters associated with NO_3^- competition were the least constrained in the model. This result was primarily due to the lack of NO_3^- pool size data, and secondarily due to the fact that NO_3^- was not the major nitrogen source for plant or decomposing microbes. We also provide quantile-based Uncertainty Reduction for reference (Table 4). The above-mentioned conclusions still hold with quantile-based UR_Q, although the quantile-based UR_Q is generally higher than variance-based UR_σ.

Convergence of model parameters is reported with the Gelman-Rubin criterion (Figure A2). Using this criterion, eleven (out of twenty) parameters are found to converge (Gelman-Rubin <= 1.1). One reason for the lack of convergence of the remaining parameters is likely data paucity and resulting equifinality. In particular, starting from different prior values, MCMC calibrations may result in different converged posteriors

but predict similar dynamics. In this regard, high frequency measurements may improve model calibration [*Tang and Zhuang*, 2008]. We acknowledge that, for large-scale model application, more work on parameter tuning and uncertainty analysis is needed. However, even with these caveats, the model predictability is reasonably good when applied to the tropical forest fertilization experiments described in Section 3.4.

We re-organize the right hand sides of Eqns. 14 – 22 to be the product of potential nutrient uptake rate and an ECA limitation term; for example for plant NH_4^+ uptake:

$$F_{NH4}^{plant} = k_{NH4}^{plant} \cdot ECA_{NH4}^{plant} \tag{32}$$

$$ECA_{NH4}^{plant} = \frac{[NH4]\cdot[E_N^{plant}]}{KM_{NH4}^{plant}(1+\frac{[NH4]}{KM_{NH4}^{plant}}+\frac{[NO3]}{KM_{NO3}^{plant}}+\frac{[E_N^{plant}]}{KM_{NH4}^{plant}}+\frac{[E_N^{mic}]}{KM_{NH4}^{mic}}+\frac{[E_N^{nit}]}{KM_{NH4}^{nit}})} \tag{33}$$

Other "consumer-substrate reactions" have similar forms. Under a nutrient abundant situation (*e.g.*, fertilized agriculture ecosystem), the relative competitiveness of each consumer (*ECA*) is dominated by its specific enzyme abundance ([*E*]). Under such conditions, substrate affinity is no longer a controlling factor. In contrast, under nutrient limited conditions (*e.g.*, many natural ecosystems), ECA is dominated by the specific enzyme abundance as well as the substrate affinity ([*E*]/*KM*). Therefore, consumers could either enable an alternative high affinity nutrient transporter system (low *KM*) or exude more enzyme to enhance competitiveness. For example, at the whole-soil scale it has been shown that root spatial occupation (C_{froot}) determines a plant's competitiveness when low soil nutrient diffusivity is limiting nutrient supply [*Raynaud and Leadley*, 2004]. Consistently, our results highlighted the dominant role of nutrient carrier enzyme abundance (*E* proportional to C_{froot}) in controlling competition. If we further assumed that plants, decomposing microbes, and nitrifiers enzyme abundances were

approximately equal, we will have that the relative their competitiveness in acquiring NH_4^+ was about 4:10:9 ($1/KM_{NH4}^{plant}:1/KM_{NH4}^{mic}:1/KM_{NH4}^{nit}$). However, such results could not be easily generalized to other ecosystems, because they heavily relied on the traits (affinity) of specific competitors. For a different ecosystem, those traits would be drastically different due to the change of, *e.g.*, plant species composition and microbial community structure. Even for the same ecosystem, those traits could be highly heterogeneous. For example, the community structure of decomposing microbes could be different in rhizosphere and bulk soil (with different *KM*). However, in this work we assumed a well-mixed environment (one soil column), in order to be consistent with large-scale ecosystem models. Although beyond the scope of the current study, the consequences of ignoring the rhizosphere versus bulk soil heterogeneity warrants further investigation. Large-scale models aim to quantify ecosystem level dynamics, although they are usually driven by parameters inferred from *in situ* field observations. In the absence of a model that explicitly represents this spatial heterogeneity, it is difficult to quantify the impacts of using inferred rhizosphere decomposer affinities on model predictions of the whole soil [*Schimel et al.*, 1989].

Our modeling framework highlights the important concept that "competitiveness" is a dynamic property of the competition network, and more importantly that it is linked to competitor functional traits (affinity and nutrient carrier enzyme abundance). This concept is in contrast to the prevailing assumption underlying all major large-scale ecosystem models, which either assume "relative demand competitiveness for different nutrient consumers" [*Thornton et al.*, 2007] or "soil microbes outcompete plants" [*McGuire et al.*, 1992; *Parton et al.*, 1988]. Imposing such pre-defined orders of

492 competitiveness neglects the diversity of nutrient competitors (plants and microbes) and
493 their differences in nutrient uptake capacity expressed by relevant functional traits. Our
494 model framework offers a theoretically consistent approach to account for the diversity of
495 nutrient competition in different competitor networks.

496 **3.2 Model sensitivity analysis**

497 Through sensitivity analysis, we separately investigated the factors controlling
498 plant NH_4^+, NO_3^-, and PO_x competition (Figure 3). Each sensitivity analysis consisted of
499 three scenarios: (1) normal conditions (control); (2) elevated soil temperature ($+T_s$); and
500 (3) elevated soil moisture ($+\theta$). The sensitivity analysis indicates that the model is highly
501 sensitive to kinetics parameters (*e.g.*, KM). Furthermore, the model is consistently
502 sensitive to the same parameters across all temperature and moisture conditions. The
503 environment affects the nutrient competition primarily through altering the nutrient
504 abundance. Enhanced soil temperature and soil moisture accelerated soil organic carbon
505 turnover, thereby releasing more inorganic nutrient into the soil (gross mineralization).
506 However, the impacts on plant nutrient uptake are limited (Figure 3) because the
507 enhanced soil organic matter decay also requires higher immobilization fluxes to sustain
508 the soil organic matter CNP stoichiometry. The enhancement of net mineralization would
509 be limited, and therefore would not change soil nutrient status dramatically.

510 **3.3 Posterior model performance**

511 The prior and posterior models were compared against observational datasets of
512 pool sizes of soil free phosphate, sorbed phosphate, and NH_4^+, CO_2 efflux, and N_2O
513 efflux (Figure 4). We note that although we attempted to acquire as many datasets that
514 contained these five observations as possible, more observations in tropical ecosystems

would clearly improve the posterior parameter estimates. For example, in the experiment we analyzed, only three measurements of soil free phosphate were made during 1999. Many detailed dynamics are therefore missing and could impact our posterior parameter estimates. The prior model predicted an increasing trend of soil free PO_x, which resulted from underestimates of plant P uptake (by underestimating of k_P^{plant}) and soil microbial P immobilization (by overestimating KM_P^{mic}). The posterior model captured the seasonal dynamics of soil free PO_x reasonably well: increases during the wet season and gradual decreasing during the dry season (August to November). The prior model also largely underestimated the seasonal variability of nitrogen dynamics and underestimated the NH_4^+ pool size due to overestimation of plant NH_4^+ uptake (k_{NH4}^{plant}). In addition, it also underestimated the denitrification N_2O emissions, because of an underestimation of NH_4^+ to NO_3^- transformation rate (k_{nit}). Consequently, there was not enough NO_3^- substrate to react with denitrifiers and release N_2O. The posterior model, however, accurately reproduced the seasonal dynamics of both NH_4^+ pool sizes and soil N_2O emissions. There were small differences between the prior and posterior model predictions of soil CO_2 emissions. The CO_2 and N_2O effluxes were more frequently observed at Tapajos National Forest during 1999 to 2001, compared with phosphorus data. Most of the measurements were collected during the wet season. Therefore the modeled CO_2 and N_2O emissions were largely improved by assimilating these datasets.

The posterior model performance implies that after assimilating multiple datasets, our model predictions were improved over the prior model. However, it is clear that more observations of the metrics applied in our MCMC approach would benefit the posterior model. Unfortunately, because of our focus on tropical sites, we were unable to acquire

more datasets that had the full suite of measurements required. Datasets of soil nutrient pool sizes (*e.g.*, NO_3^-) and higher frequency sampling of those sparse measurements (*e.g.*, POx) would significantly benefit the model uncertainty reduction.

3.4 Model testing against nitrogen and phosphorus fertilization studies

To test the posterior N-COM model, we conducted short-term numerical competition experiments (24-hour or 48-hour simulations) by manually imposing an input flux into nutrient pools equivalent to the N and P fertilization experiments described above and in Table 5. The simulated results were compared with observations from the field manipulations.

In the P addition experiments across the Hawaiian chronosequence, the partitioning of phosphate between microbes and mineral surfaces was well represented by the N-COM model in the intermediate (20K yr) and old (4.1M yr) sites (Figures 5b and 5c), with no significant differences between model predictions and observations. In the youngest Hawaiian site (300 yr; Figure 5a), the relative partitioning was correctly simulated, but the predicted PO_4^{3-} magnitudes were lower than observations. Our simulations indicated that at the young soil site the added P exceeded microbial demand, resulting in lower predicted microbial P uptake than observed. This discrepancy reflected a possible deficiency of first-order SOC decay models (as we used here), which implicitly treat microbes as a part of soil organic matter. Since microbial nutrient immobilization is strictly regulated by the SOC turnover rate in this type of model, external nutrient inputs will no longer affect microbial nutrient uptake if the inputs exceed potential microbial demand. We therefore believe that explicit Microbe-Enzyme models might be able to better explain the strong microbe PO_4^{3-} uptake signal observed at the young Hawaii

561 fertilization experiment site. Microbial models explicitly simulate the dynamics of
562 microbial biomass, which might be able to capture the expected rapid growth of
563 microbial communities under conditions of improved substrate quality [*Kaspari et al.*,
564 2008; *Wieder et al.*, 2009].

565 In the Puerto Rican Luquillo forest nitrogen addition experiments, partitioning of
566 added ammonium between plants and heterotrophic bacteria was well captured by the N-
567 COM model, with no significant differences between model predictions and observations
568 (Figure 5d). However, the model underestimated nitrifier NH_4^+ uptake. NO_3^- competition
569 in this site was also relatively accurately predicted (Figure 5e), although the
570 measurements did not include denitrification. Model estimates of plant NO_3^- uptake and
571 microbial NO_3^- immobilization were consistent with the observed ranges, but we
572 highlight the large observational uncertainties, particularly for microbial NO_3^- uptake.

573 In the pseudo-first-order decomposition model we applied here to demonstrate the
574 ECA competition methodology, the soil organic matter C:N:P ratio also limited microbial
575 N and P uptake. For this type of decomposition model, stoichiometric differences
576 between soil organic matter and microbes are not dynamically simulated. Such a
577 simplification of soil and microbial stoichiometry favors large spatial scale model
578 structures over long temporal periods, but hampers prediction of microbial short-term
579 responses to N and P fertilization. For example, the observed difference between
580 microbial and soil C:P ratios can be as large as 6-fold [*Mooshammer et al.*, 2014; *Xu et*
581 *al.*, 2013]. Were that the case in the observations we applied, the potential soil P demand
582 calculated based on a fixed soil organic matter C:P ratio could be only 17% of that based
583 on microbial C:P ratio.

584 **3.5 Implications of ECA competition treatment**

585 Terrestrial ecosystem growth and function are continuously altered by climate
586 (*e.g.*, warming, drought; [*Chaves et al.*, 2003; *Springate and Kover*, 2014]), external
587 nutrient inputs (*e.g.*, N deposition; [*Matson et al.*, 2002; *Matson et al.*, 1999]), and
588 atmospheric composition (*e.g.*, CO_2 concentration; [*Norby et al.*, 2010; *Oren et al.*, 2001;
589 *Reich et al.*, 2006]). Improved understanding of the underlying mechanisms regulating
590 ecosystem responses to environmental changes has been obtained through *in situ* level to
591 large-scale and long-term manipulation experiments. For example, decade-long Free-Air
592 Carbon Dioxide Enrichment (FACE) experiments have revealed that nitrogen limitation
593 diminished the CO_2 fertilization effect of forests [*Norby et al.*, 2010] and grasslands
594 [*Reich and Hobbie*, 2013] ecosystems. However, fewer efforts have been made towards
595 incorporating the observed process-level knowledge into Earth System Models (ESMs).
596 Therefore, a major uncertainty that has limited the predictability of ESMs has been the
597 incomplete representation of soil nutrient dynamics [*Zaehle et al.*, 2014]. Even though
598 new soil nutrient cycle paradigms were proposed during recent decades [*Korsaeth et al.*,
599 2001; *Schimel and Bennett*, 2004], they were restricted to either conceptual models or
600 only applied to explain laboratory experiments.

601 Many large-scale terrestrial biogeochemistry models (*e.g.*, O-CN, CASA, TEM)
602 have adopted the classical paradigm that microbes decompose soil organic matter and
603 release NH_4^+ as a "waste" product [*Waksman*, 1931]. The rate of this process is defined
604 as "net N mineralization", and is adopted as a "measure" of plant available inorganic N
605 [*Schimel and Bennett*, 2004]. This classical paradigm overlooked the fact that "net N
606 mineralization" actually comprised two individual processes - gross N mineralization and

607 microbial N immobilization. Implicitly, the classical paradigm assumes that the microbes
608 have priority to assimilate as much of the available nutrient pool as possible. Soil
609 nutrients were only available for plant uptake if there were not enough free energy
610 materials (*e.g.*, dissolved soil organic carbon) to support microbial metabolism. As a
611 result, soil microbes were considered "victors" in the short-term nutrient competition.
612 Some other large-scale terrestrial biogeochemistry models (*e.g.*, CLM4CN), simplify the
613 concept of nutrient competition differently. They calculate the plant N uptake and soil N
614 immobilization separately; and then down-regulate the two fluxes according to the soil
615 mineral N availability. As a result, plant and soil microbe competitiveness for nutrients is
616 determined by their relative demand.

617 Climate-scale land models have over-simplified or ignored competition between
618 plants, microbes, and abiotic mechanisms. In reality, under high nutrient stress
619 conditions, plants can exude nutrient carrier enzymes or facilitate mycorrhizal fungi
620 associations to enhance competitiveness for nutrient acquisition [*Drake et al.*, 2011;
621 *Hobbie and Hobbie*, 2006; *Treseder and Vitousek*, 2001]. In addition, plants can adjust C
622 allocation to construct more fine roots, which scavenge nutrients over larger soil volumes
623 [*Iversen et al.*, 2011; *Jackson et al.*, 2009; *Norby et al.*, 2004]. Soil spatial heterogeneity
624 might also contribute to the success of plant nutrient competition [*Korsaeth et al.*, 2001].
625 Therefore, most ecosystem biogeochemistry models with traditional treatments of
626 nutrient competition likely underestimate plant nutrient uptake.

627 Nutrient competition should be treated as a complex consumer-substrate reaction
628 network: multiple 'consumers', including plant roots, soil heterotrophic microbes,
629 nitrifiers, denitrifiers, and mineral surfaces, each competing for substrates of organic and

630 inorganic nitrogen and phosphorus as nutrient supply. In such a model structure, the
631 success of any consumer in substrate acquisition is affected by its consumer-substrate
632 affinity [*Nedwell*, 1999]. Such competitive interactions have been successfully applied to
633 microbe-microbe and plant-microbe substrate competition modeling [*Bonachela et al.*,
634 2011; *Lambers et al.*, 2009; *Maggi et al.*, 2008; *Maggi and Riley*, 2009; *Moorhead and*
635 *Sinsabaugh*, 2006; *Reynolds and Pacala*, 1993] for many years.
636 Here, we applied the consumer-substrate network in a broader context of plant,
637 microorganism, and abiotic mineral interactions. We analyzed the consumer-substrate
638 network using a first-order accurate equilibrium chemistry approximation (ECA) [*Tang*
639 *and Riley*, 2013; *Zhu and Riley*, 2015]. Our sensitivity analysis confirmed that the
640 consumer-substrate affinity and nutrient carrier enzyme abundance were the most
641 important factors regulating relatively short-term competitive interactions. The ECA
642 competition treatment represents ecosystem responses to environmental changes and has
643 the potential to be linked to a microbe-explicit land biogeochemistry model. The
644 approach allows competition between plants, microbes, and mineral surfaces to be
645 prognostically determined based on nutrient status and capabilities of each consumer.
646

647 **4. Conclusions**

648 In this study, we developed a soil biogeochemistry model (N-COM) that resolves
649 the dynamics of soil nitrogen and phosphorus, plant uptake of nutrients, microbial uptake,
650 and abiotic interactions. We focused on the implementation, parameterization, and testing
651 of the nutrient competition scheme that we plan to incorporate into the ESM land models
652 CLM and ALM. We described the multiple-consumer and multiple-nutrient competition

653 network with the Equilibrium Chemical Approximation (ECA) [*Tang and Riley*, 2013]
654 considering two inhibitive effects: (1) multiple substrates (*e.g.*, NH_4^+ and NO_3^-) sharing
655 one consumer inhibits the effective binding between any specific substrate and the
656 consumer and (2) multiple consumers (*e.g.*, plants, decomposing microbes, nitrifers)
657 sharing one substrate (*e.g.*, NH_4^+) lowers the probability of effective binding between any
658 consumer and that substrate. We calibrated the model at a tropical forest site with highly
659 weathered soil (Tapajos National Forest, Para, Brazil), using multiple observational
660 datasets with the Markov Chain Monte Carlo (MCMC) approach. The model parameters
661 were well constrained compared with their prior distributions (Table 4). The posterior
662 parameter uncertainties were greatly reduced (on average by 75%). The posterior model
663 compared to multiple categories of observational data was substantially improved over
664 the prior model (Figure 4). The seasonal dynamics of soil carbon, nitrogen, and
665 phosphorus were moderately well captured. However, our results would likely be more
666 robust if more temporally resolved observations of carbon, nitrogen, and phosphorous
667 were available in the individual consumer pools.
668 To test the resulting model using the posterior parameters, we applied N-COM to
669 two other tropical forests (Hawaii tropical forest and Luquillo tropical forest) not used in
670 the calibration process and conducted nutrient perturbation studies consistent with
671 fertilization experiments at these sites. The results showed that N-COM simulated the
672 nitrogen and phosphorus competition well for the majority of the observational metrics.
673 However, the model underestimated NH_4^+ uptake by nitrifiers, probably due to the
674 loosely constrained nitrification parameters that were the result of NO_3^- pool size data
675 paucity during calibration at the Brazil site (Table 4). Datasets of soil nutrient pool sizes

676 and CO_2 and N_2O effluxes with high frequency sampling would significantly benefit the
677 model uncertainty reduction.

678 To date, many terrestrial ecosystem biogeochemistry models assume microbes
679 outcompete plants and immobilize nutrients first [*Y P Wang et al.*, 2007; *Zaehle and*
680 *Friend*, 2010; *Zhu and Zhuang*, 2013], although CLM currently assumes constant and
681 relative demand competitiveness of plants and microbes. Few models, to our knowledge,
682 consider the role of abiotic interactions in the competitive interactions. In the case of
683 microbes outcompeting plants, the plant is only able to utilize the nutrients that exceed
684 microbial demands during that time step. The leftover nutrients are defined as net
685 mineralization, which is a widely adopted concept in soil biogeochemistry modeling
686 [*Schimel and Bennett*, 2004]. These models oversimplify plant-microbe interactions by
687 imposing dubious assumptions (*e.g.*, microbes always win against plants). We showed
688 that (in section 3.1) "competitiveness" is a dynamic rather than fixed property of the
689 competition network, and more importantly, it should be linked to competitor functional
690 traits (affinity and nutrient carrier enzyme abundance).

691 This study is an important step towards implementing more realistic nutrient
692 competition schemes in complex climate-scale land models. Traditional ESMs generally
693 lack realistic soil nutrient competition, which likely biases the estimates of terrestrial
694 ecosystem carbon productivity and biosphere-climate feedbacks. This study showed the
695 effectiveness of ECA kinetics in representing soil multiple-consumer and multiple-
696 nutrient competition networks. Offline calibration and independent site-level testing is
697 critically important to ensuring the newly incorporated model will perform reasonably
698 when integrated in a complex ESM. To this end, we provide a universal calibration

699 approach using MCMC, which could in the future be used to further constrain N-COM
700 across plant functional types, climate, and soil types.
701
702 *Acknowledgements:* This research was supported by the Director, Office of Science,
703 Office of Biological and Environmental Research of the US Department of Energy under
704 Contract No. DE-AC02-05CH11231 as part of the Regional and Global Climate
705 Modeling (RGCM) and ACME programs.

Figure 1. Model structure. Boxes represent pools, solid arrows represent aqueous fluxes, and dashed arrows represent gaseous pathways out or into the system. Three essential chemical elements (Carbon (C), Nitrogen (N) and Phosphorus (P)) are simulated in N-COM (blue, red, and green represent C, N, and P pools and processes, respectively).

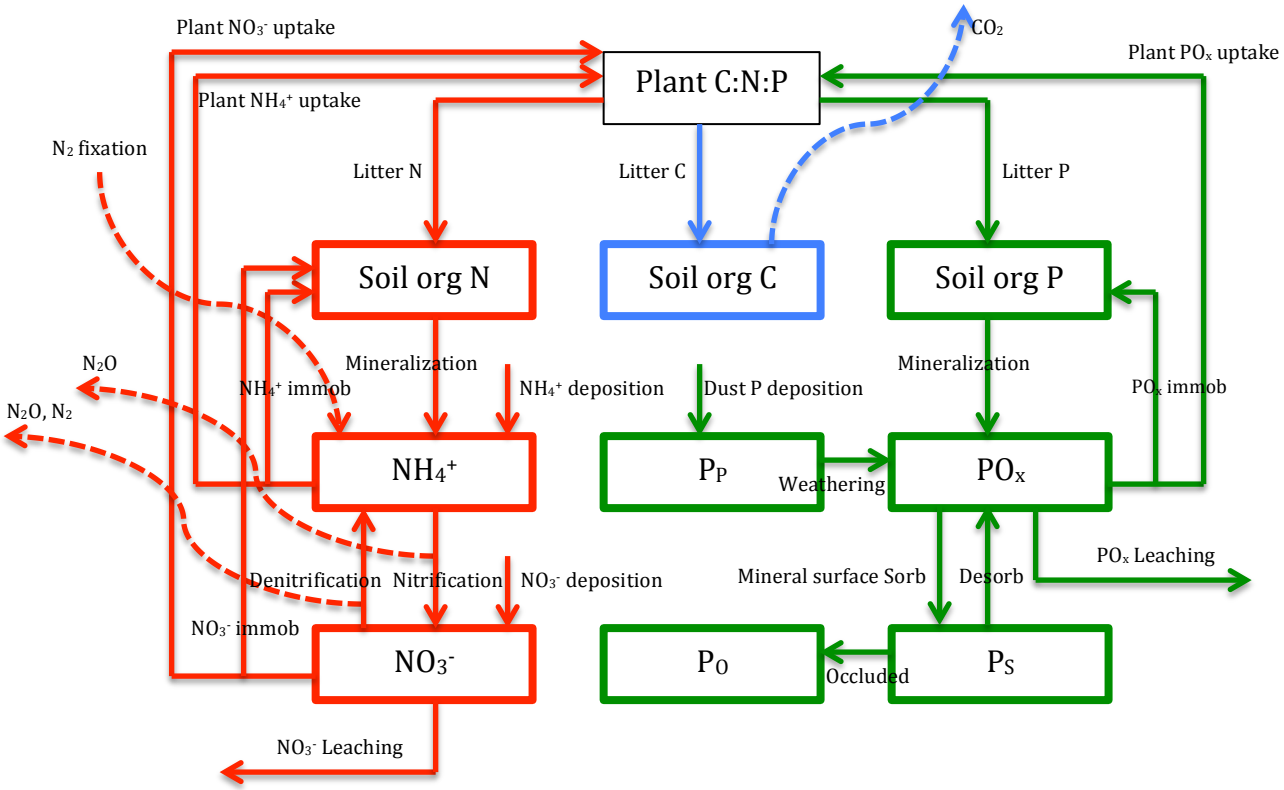

Figure 2. Distribution of prior and posterior model parameters.

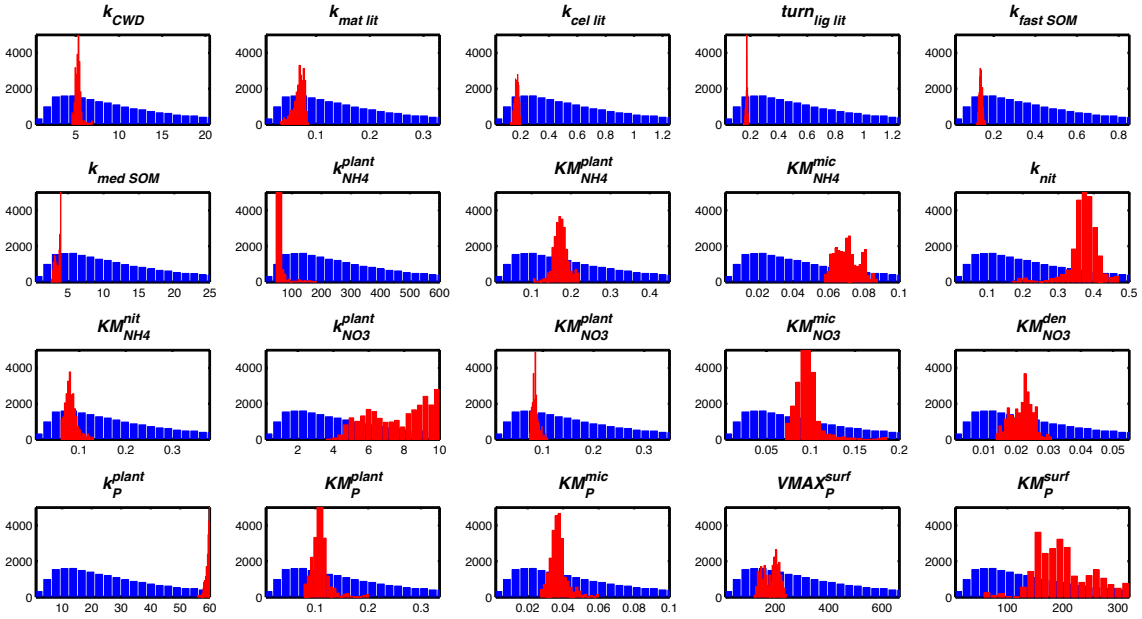

Figure 3. Model sensitivity analysis with SOBOL sampling. For each metric, three scenarios are shown: baseline (Control), elevated soil temperature by 5 °C ($+T_s$), and elevated soil moisture by 50% ($+\theta$), respectively. The length of bar (plot in polar coordinate) is the sensitivity (unit-less) of model output with respect to model input variables. Our results showed that the plant nutrient uptake was mostly regulated by internal consumer-substrate uptake kinetics rather than the external environmental conditions (*e.g.*, T_s, θ).

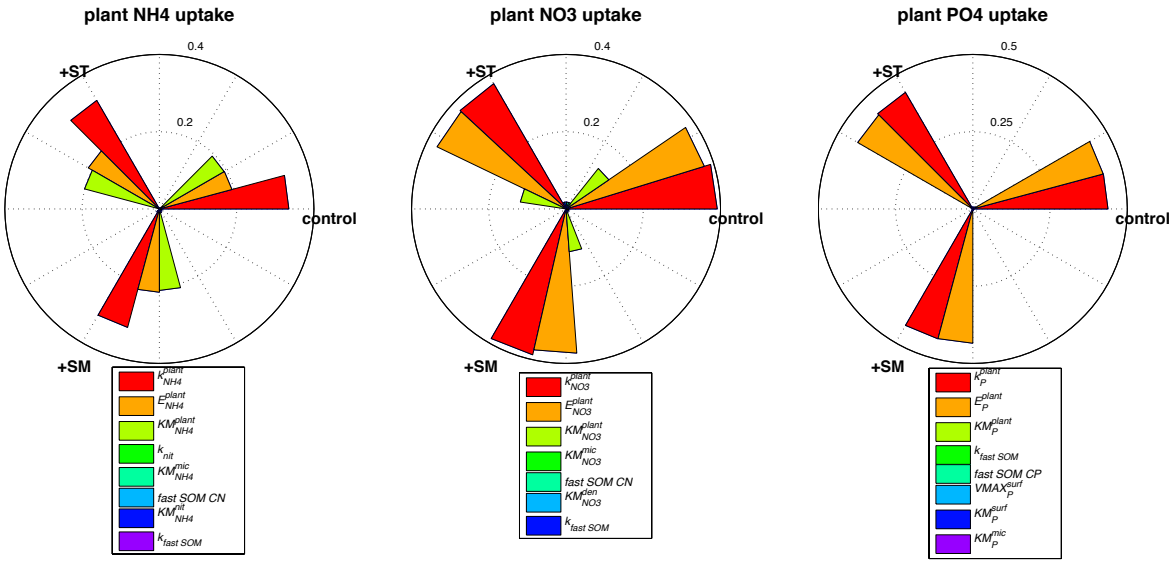

Figure 4. Model performance at Tapajos National Forest, Para, Brazil. Overall, the posterior model (blue line) improved predictions over the prior model (grey line) when compared to observations. Green areas indicate the posterior model uncertainties.

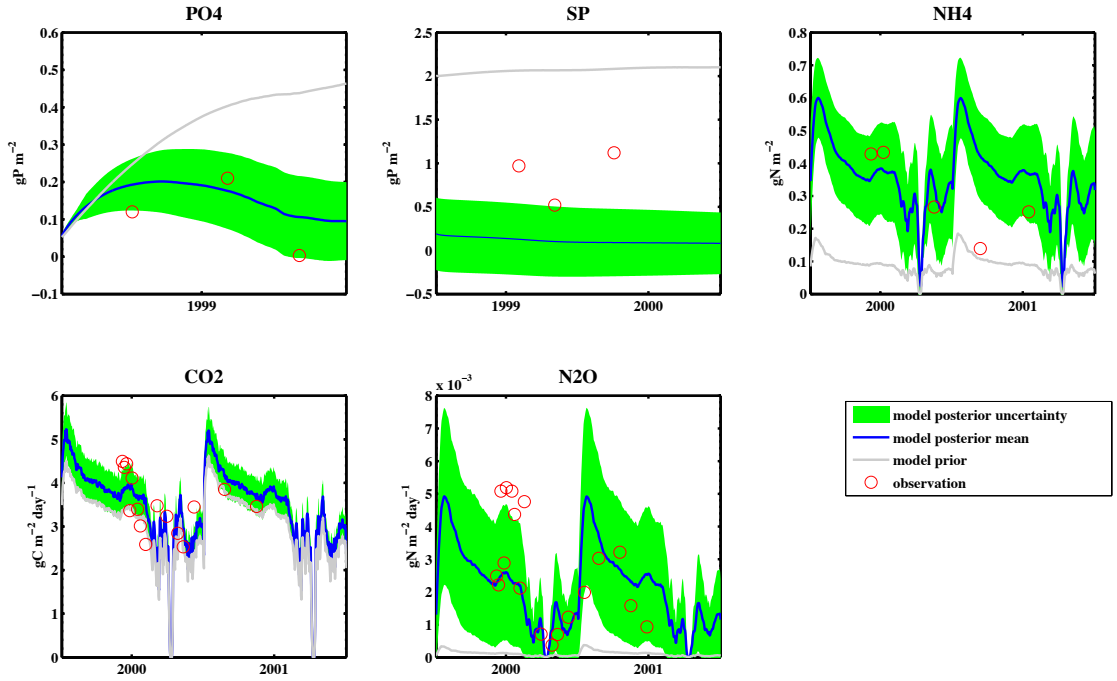

Figure 5. Model perturbation experiments compared with nitrogen and phosphorus fertilization field experimental data. The blue dots show the difference between control and perturbed simulations, which mean how much newly added nutrient each consumer takes up. The red circles are recovered isotopically labeled nutrient within each consumer. Since plants phosphorus uptake was not measured at Hawaii sites, we didn't include the plants in the perturbation study.

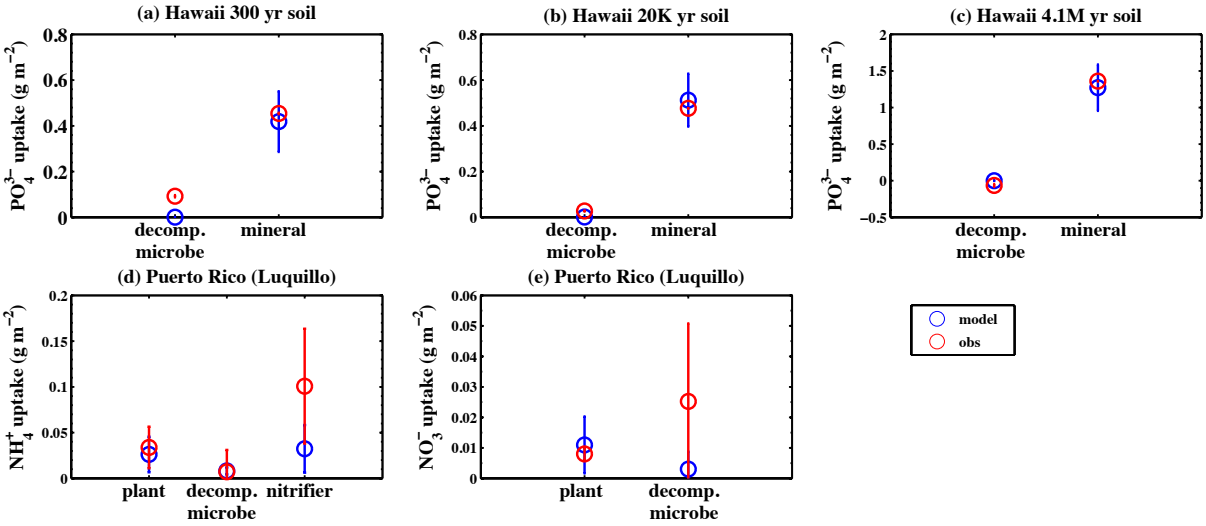

732 **Table 1.** A summary of the modeled consumer-resource competition network.

Resources	**Consumers**		
NH_4^+	Plant	Decomposing Microbe	Nitrifier
NO_3^-	Plant	Decomposing Microbe	Denitrifier
PO_x	Plant	Decomposing Microbe	Mineral surface

733

734 **Table 2.** Model parameters and baseline values.

C associated				
g_i	Percentage of carbon remains in the soil after decomposition of i^{th} SOM	-	[1.0; 0.45; 0.5; 0.5; 0.83; 0.45; 0.45]	[*Koven et al.*, 2013]
f_{ij}	fraction of SOM leave from i^{th} pool and enter into j^{th} pool	-	[0, 0, 0.76, 0.24, 0, 0, 0; 0, 0, 0, 0, 1, 0, 0; 0, 0, 0, 0, 1, 0, 0; 0, 0, 0, 0, 0, 1, 0; 0, 0, 0, 0, 0, 0.995, 0.005; 0, 0, 0, 0, 0.93, 0, 0.07; 0, 0, 0, 0, 1, 0, 0]	[*Koven et al.*, 2013]
CN	Soil organic matter CN ratio	-	[13,16,7.9]	[*Parton et al.*, 1988]
CP	Soil organic matter CP ratio	-	[110,320,114]	[*Parton et al.*, 1988]
$TURN_{SOM}$	Soil organic matter turn over [CWD, metabolic lit, cellulose lit, lignin lit, fast SOM, medium SOM, slow SOM]	year	[4.1, 0.066, 0.25, 0.25, 0.17, 5, 270]	[*Koven et al.*, 2013]
N associated				
k_{NH4}^{plant}	Reaction rate of plant NH_4^+ carrier enzyme	day^{-1}	120 (a)	[*Jackson et al.*, 1997; *Min et al.*, 2000]
KM_{NH4}^{plant}	Half-saturation constant for plant NH_4^+ uptake	$g\ m^{-2}$	0.09	[*Kuzyakov and Xu*, 2013]
KM_{NH4}^{mic}	Half-saturation constant for decomposing microbe NH_4^+ immobilization	$g\ m^{-2}$	0.02	[*Kuzyakov and Xu*, 2013]
k_{nit}	Maximum fraction of NH_4^+ pool that could be utilized by nitrifiers	day^{-1}	10%	[*Parton et al.*, 2001]
KM_{NH4}^{nit}	Half-saturation constant for nitrifier NH_4^+ consumption	$g\ m^{-2}$	0.076	[*Drtil et al.*, 1993]
k_{NO3}^{plant}	Reaction rate of plant NO_3^- carrier enzyme	day^{-1}	2 (a)	[*Jackson et al.*, 1997; *Min et al.*, 2000]
KM_{NO3}^{plant}	Half-saturation constant for plant NO_3^- uptake	$g\ m^{-2}$	0.07	[*Kuzyakov and Xu*, 2013]
KM_{NO3}^{mic}	Half-saturation constant for decomposing microbe NO_3^- immobilization	$g\ m^{-2}$	0.04	[*Kuzyakov and Xu*, 2013]
KM_{NO3}^{den}	Half-saturation constant for denitrifier NO_3^- consumption	$g\ m^{-2}$	0.011	[*Murray et al.*, 1989]
$[E_N^{plant}]$	Plant nitrogen carrier enzyme abundance for nitrogen uptake	$g\ m^{-2}$	$C_{froot} \cdot 0.0000125$ (a)	[*Tang and Riley*, 2013; *Trumbore et al.*, 2006]
$[E_N^{mic}]$	Decomposing microbes nitrogen carrier enzyme abundance for nitrogen immobilization	$g\ m^{-2}$	$\frac{F_N^{immob,pot}}{1000}$ (b)	[*Tang and Riley*, 2013]
$[E_N^{nit}]$	Nitrifier nitrogen carrier enzyme abundance for NH_4^+ assimilation	$g\ m^{-2}$	$1.2E^{-3}$	[*Raynaud et al.*, 2006]

$[E_N^{den}]$	Denitrifier nitrogen carrier enzyme abundance for NO_3^- assimilation	g m^{-2}	1.2E^{-3}	[*Raynaud et al.*, 2006]
f^{N2O}	Fraction of nitrification flux lost as N_2O	-	6E^{-4}	[*Li et al.*, 2000]
P associated				
$k_{weather}$	Parent material P weathering rate	g P m^{-2} year^{-1}	0.004	[*Y P Wang et al.*, 2010]
k_{occl}	P occlude rate	month^{-1}	1.0E^{-6}	[*Yang et al.*, 2014]
k_P^{plant}	Reaction rate of plant PO_x carrier enzyme	day^{-1}	12 (a)	[*Colpaert et al.*, 1999]
KM_P^{plant}	Half-saturation constant for plant PO_x uptake	g m^{-2}	0.067	[*Cogliatti and Clarkson*, 1983]
KM_P^{mic}	Half-saturation constant for decomposing microbe PO_x immobilization	g m^{-2}	0.02	[*Chen*, 1974]
$VMAX_P^{surf}$	Maximum mineral surface PO_x adsorption	g m^{-2}	133	[*Y P Wang et al.*, 2010]
KM_P^{surf}	Half-saturation constant for mineral surface PO_x adsorption	g m^{-2}	64	[*Y P Wang et al.*, 2010]
$[E_P^{plant}]$	Plant phosphorus carrier enzyme abundance for PO_x uptake	g m^{-2}	$C_{froot} \cdot 0.0000125$ (a)	[*Tang and Riley*, 2013; *Trumbore et al.*, 2006]
$[E_P^{mic}]$	Decomposing microbes phosphorus carrier enzyme abundance for PO_x immobilization	g m^{-2}	$\frac{F_P^{immob,pot}}{800}$ (b)	[*Tang and Riley*, 2013]
$[E_P^{surf}]$	Mineral surface "effective enzyme" abundance for PO_x adsorption	g m^{-2}	$VMAX_P^{surf} - [SP]$	[*Tang and Riley*, 2013]

(a) The scaling factor for plant nutrient enzyme abundance is 0.0000125. This number is inferred by assuming that growing season plant nutrient carrier enzymes are roughly the same order of magnitude compared with decomposing microbes'. Typical values for soil decomposing microbe biomass and tropical forest fine root biomass are 0.1 [*Tang and Riley*, 2013] and 400 [*Trumbore et al.*, 2006] gC m^{-2}. A typical value of scaling factor that scales microbial biomass to enzyme abundance is 0.05 [*Tang and Riley*, 2013]. Therefore, $C_{froot} \cdot x = C_{mic} \cdot 0.05$ or $400 \cdot x = 0.1 \cdot 0.05$. We have $x = 0.0000125$. Further, we have $k_{NH4}^{plant} \cdot [E_N^{plant}] = VMAX_{NH4}^{plant}$. We know that typical values for $VMAX_{NH4}^{plant}$ and $[E_N^{plant}]$ are 0.6 g m^{-2} day^{-1} [*Min et al.*, 2000] and 0.005 g m^{-2}. Then we have $k_{NH4}^{plant} = 120$ day^{-1}. Similarly, we have $k_{NO3}^{plant} \cdot [E_N^{plant}] = VMAX_{NO3}^{plant}$, $k_P^{plant} \cdot [E_P^{plant}] = VMAX_P^{plant}$. Knowing that typical values for $VMAX_{NO3}^{plant}$ and $VMAX_P^{plant}$ are 0.01 [*Min et al.*, 2000] and 0.06 [*Colpaert et al.*, 1999] g m^{-2} day^{-1}, we have $k_{NO3}^{plant} = 2$ and $k_P^{plant} = 12$ day^{-1}.

(b) For decomposing microbes, we have $VMAX_N^{mic} = k_N^{mic} \cdot [E^{mic}{}_N]$. Typical values for $VMAX_N^{immob}$ and $[E_N^{mic}]$ are 5 g m^{-2} day^{-1} [*Kuzyakov and Xu*, 2013] and 0.005 g m^{-2} [*Tang and Riley*, 2013]. Therefore, we have $k_N^{mic} = 1000$. Since our model calculates potential N immobilization rates and approximates them as $VMAX_N^{mic}$. The changes of potential N immobilization rates at each time step imply the changes of enzyme abundance through $[E_N^{mic}] = \frac{F_N^{immob,pot}}{k_N^{mic}} = \frac{F_N^{immob,pot}}{1000}$. Similarly, we have that $VMAX_P^{immob}$ and $[E_N^{mic}]$ are 2 g m^{-2} day^{-1} [*Chen*, 1974] and 0.005 g m^{-2}. Therefore, $k_P^{mic} = 800$ and $E_P^{mic} = \frac{F_P^{immob,pot}}{800}$.

735 **Table 3.** Observational datasets used for calibration. Number of observations for each

736 data stream is included in brackets.

Processes	Datasets		Location	References
C associated	Soil heterotrophic respiration (20)		Tapajos National Forest, Para, Brazil	[*Silver et al.*, 2012]
N associated	Soil NH_4^+ (5)	N_2O efflux (20)	Tapajos National Forest, Para, Brazil	[*Silver et al.*, 2012]
P associated	Soil free phosphate (3)	Sorb phosphate (3)	Tapajos National Forest, Para, Brazil	[*McGroddy et al.*, 2008]

737

Table 4. Posterior parameters are reported in terms of (1) mean/standard deviation by fitting to a Gaussian distribution; (2) 25% and 75% quantile. Both variance-based and quantile-based parameters uncertainty reduction are provided.

Parameters	μ_{prior}	σ_{prior}	$\mu_{posterior}$	$\sigma_{posterior}$	**UR**	Q^{25}_{prior}	Q^{75}_{prior}	$Q^{25}_{posterior}$	$Q^{75}_{posterior}$	**UR**
$TURN_{SOM}$	[3.7,	[3.9,	[5.2,	[0.33,	[92,	[5.33,	[19.32,	[5.05, 0.63,	[5.39,	[97,
[CWD,	0.06,	0.06,	0.07,	0.01,	83,	0.086,	0.31,	0.16, 0.17,	0.076, 0.18,	94,
metabolic,	0.23,	0.24,	0.17,	0.01,	96,	0.33,	1.18,	0.13, 3.2]	0.18, 0.14,	97,
cellulose,	0.23,0.16,	0.24,	0.17,	0.005,	98,	0.33,	1.18,		3.9]	99,
lignin lit,	4.6]	0.18,	0.14,	0.008,	96,	0.22,	0.8,			98, 96
fast,		4.8]	3.6]	0.37]	92]	6.5]	23.5]			
medium										
SOM]										
k_{NH4}^{plant}	109	114	58	14	88	156.1	565.4	52.8	60.0	98
KM_{NH4}^{plant}	0.082	0.086	0.173	0.018	79	0.12	0.42	0.16	0.18	93
KM_{NH4}^{mic}	0.018	0.019	0.071	0.0067	65	0.026	0.094	0.065	0.076	85
k_{nit}	0.091	0.095	0.37	0.038	60	0.13	0.47	0.36	0.39	91
KM_{NH4}^{nit}	0.069	0.072	0.082	0.012	83	0.10	0.36	0.07	0.09	94
k_{NO3}^{plant}	1.8	1.9	7.6	1.7	13	2.60	9.42	6.11	9.14	56
KM_{NO3}^{plant}	0.064	0.067	0.085	0.0064	90	0.09	0.33	0.08	0.09	97
KM_{NO3}^{mic}	0.036	0.038	0.096	0.014	63	0.05	0.19	0.09	0.10	92
KM_{NO3}^{den}	0.0101	0.0105	0.022	0.0034	68	0.014	0.052	0.019	0.024	87
k_{P}^{plant}	11	11.5	59	0.75	93	15.61	56.54	58.86	59.81	98
KM_{P}^{plant}	0.061	0.064	0.11	0.015	77	0.09	0.32	0.10	0.12	94
KM_{P}^{mic}	0.018	0.019	0.037	0.0047	75	0.026	0.094	0.034	0.039	93
$VMAX_{P}^{surf}$	121	127	182	30	76	173.0	626.6	156.5	206.3	89

KM_P^{surf}	64	58	200	50	18	83.2	301.5	162.6	233.0	68

741

742 **Table 5.** Short-term (24 or 48 hours) fertilization experiments of NH_4^+, NO_3^-, or PO_4^{3-}

743 additions used to evaluate the performance of the N-COM competition scheme.

Datasets	**Added nutrient**	**Competitors**			**Duration (hour)**	**References**
PO_4^{3-} fertilization	10 μg g^{-1}	I. Mineral surface	II. Decomposing microbe		48	[*Olander and Vitousek*, 2005]
NH_4^+ fertilization	4.6 μg g^{-1}	I. Plant	II. Decomposing microbe	III. Nitrifier	24	[*Templer et al.*, 2008]
NO_3^- fertilization	0.92 μg g^{-1}	I. Plant	II. Decomposing microbe		24	[*Templer et al.*, 2008]

744

References:

Anav, A., P. Friedlingstein, M. Kidston, L. Bopp, P. Ciais, P. Cox, C. Jones, M. Jung, R. Myneni, and Z. Zhu (2013), Evaluating the land and ocean components of the global carbon cycle in the CMIP5 Earth System Models, *Journal of Climate*, *26*(18), 6801-6843.

Bonachela, J. A., M. Raghib, and S. A. Levin (2011), Dynamic model of flexible phytoplankton nutrient uptake, *Proceedings of the National Academy of Sciences*, *108*(51), 20633-20638.

Bonan, G. B., and K. V. Cleve (1992), Soil temperature, nitrogen mineralization, and carbon source-sink relationships in boreal forests, *Canadian Journal of Forest Research*, *22*(5), 629-639.

Chauhan, B. S., J. W. B. Stewart, and E. A. Paul (1981), Effect of labile inorganic phosphate status and organic carbon additions on the microbial uptake of phosphorus in soils, *Canadian Journal of Soil Science*, *61*(2), 373-385.

Chaves, M. M., J. P. Maroco, and J. S. Pereira (2003), Understanding plant responses to drought—from genes to the whole plant, *Functional plant biology*, *30*(3), 239-264.

Chen, M. (1974), Kinetics of phosphorus absorption byCorynebacterium bovis, *Microbial ecology*, *1*(1), 164-175.

Cogliatti, D. H., and D. T. Clarkson (1983), Physiological changes in, and phosphate uptake by potato plants during development of, and recovery from phosphate deficiency, *Physiologia plantarum*, *58*(3), 287-294.

Colpaert, J. V., K. K. Van Tichelen, J. A. Van Assche, and A. Van Laere (1999), Short-term phosphorus uptake rates in mycorrhizal and non-mycorrhizal roots of intact Pinus sylvestris seedlings, *New Phytologist*, *143*(3), 589-597.

DeLuca, T. H., O. Zackrisson, M. J. Gundale, and M.-C. Nilsson (2008), Ecosystem feedbacks and nitrogen fixation in boreal forests, *Science*, *320*(5880), 1181-1181.

DeLuca, T. H., O. Zackrisson, M.-C. Nilsson, and A. Sellstedt (2002), Quantifying nitrogen-fixation in feather moss carpets of boreal forests, *Nature*, *419*(6910), 917-920.

Dise, N. B., and R. F. Wright (1995), Nitrogen leaching from European forests in relation to nitrogen deposition, *Forest Ecology and Management*, *71*(1), 153-161.

Drake, J. E., A. Gallet‐Budynek, K. S. Hofmockel, E. S. Bernhardt, S. A. Billings, R. B. Jackson, K. S. Johnsen, J. Lichter, H. R. McCarthy, and M. L. McCormack (2011), Increases in the flux of carbon belowground stimulate nitrogen uptake and sustain the long‐term enhancement of forest productivity under elevated CO2, *Ecology letters*, *14*(4), 349-357.

Drtil, M., P. Nemeth, and I. Bodik (1993), Kinetic constants of nitrification, *Water Research*, *27*(1), 35-39.

Elser, J. J., M. E. S. Bracken, E. E. Cleland, D. S. Gruner, W. S. Harpole, H. Hillebrand, J. T. Ngai, E. W. Seabloom, J. B. Shurin, and J. E. Smith (2007), Global analysis of nitrogen and phosphorus limitation of primary producers in freshwater, marine and terrestrial ecosystems, *Ecology letters*, *10*(12), 1135-1142.

790 Friedlingstein, P., P. Cox, R. Betts, L. Bopp, W. Von Bloh, V. Brovkin, P. Cadule, S.
791 Doney, M. Eby, and I. Fung (2006), Climate-carbon cycle feedback analysis:
792 Results from the C4MIP model intercomparison, *Journal of Climate*, *19*(14),
793 3337-3353.
794 Hobbie, J. E., and E. A. Hobbie (2006), 15N in symbiotic fungi and plants estimates
795 nitrogen and carbon flux rates in arctic tundra, *Ecology*, *87*(4), 816-822.
796 Hodge, A., and A. H. Fitter (2010), Substantial nitrogen acquisition by arbuscular
797 mycorrhizal fungi from organic material has implications for N cycling,
798 *Proceedings of the National Academy of Sciences*, *107*(31), 13754-13759.
799 Hodge, A., D. Robinson, and A. Fitter (2000a), Are microorganisms more effective
800 than plants at competing for nitrogen?, *Trends in plant science*, *5*(7), 304-308.
801 Hodge, A., J. Stewart, D. Robinson, B. S. Griffiths, and A. H. Fitter (2000b),
802 Competition between roots and soil micro‐organisms for nutrients from
803 nitrogen‐rich patches of varying complexity, *Journal of Ecology*, *88*(1), 150-
804 164.
805 Houghton, R. A. (2003), Revised estimates of the annual net flux of carbon to the
806 atmosphere from changes in land use and land management 1850–2000,
807 *Tellus B*, *55*(2), 378-390.
808 Hu, S., F. S. Chapin, M. K. Firestone, C. B. Field, and N. R. Chiariello (2001), Nitrogen
809 limitation of microbial decomposition in a grassland under elevated CO2,
810 *Nature*, *409*(6817), 188-191.
811 Iversen, C. M., T. D. Hooker, A. T. Classen, and R. J. Norby (2011), Net mineralization
812 of N at deeper soil depths as a potential mechanism for sustained forest
813 production under elevated [CO2], *Global change biology*, *17*(2), 1130-1139.
814 Jackson, R. B., C. W. Cook, J. S. Pippen, and S. M. Palmer (2009), Increased
815 belowground biomass and soil CO2 fluxes after a decade of carbon dioxide
816 enrichment in a warm-temperate forest, *Ecology*, *90*(12), 3352-3366.
817 Jackson, R. B., H. A. Mooney, and E. D. Schulze (1997), A global budget for fine root
818 biomass, surface area, and nutrient contents, *Proceedings of the National*
819 *Academy of Sciences*, *94*(14), 7362-7366.
820 Ji, D., et al. (2014), Description and basic evaluation of Beijing Normal University
821 Earth System Model (BNU-ESM) version 1, *Geosci. Model Dev.*, *7*(5), 2039-
822 2064, doi:10.5194/gmd-7-2039-2014.
823 Johnson, D. W. (1992), Nitrogen retention in forest soils, *Journal of Environmental*
824 *Quality*, *21*(1), 1-12.
825 Kaspari, M., M. N. Garcia, K. E. Harms, M. Santana, S. J. Wright, and J. B. Yavitt (2008),
826 Multiple nutrients limit litterfall and decomposition in a tropical forest,
827 *Ecology Letters*, *11*(1), 35-43.
828 Kaye, J. P., and S. C. Hart (1997), Competition for nitrogen between plants and soil
829 microorganisms, *Trends in Ecology & Evolution*, *12*(4), 139-143.
830 Korsaeth, A., L. Molstad, and L. R. Bakken (2001), Modelling the competition for
831 nitrogen between plants and microflora as a function of soil heterogeneity,
832 *Soil Biology and Biochemistry*, *33*(2), 215-226.
833 Koven, C. D., W. J. Riley, Z. M. Subin, J. Y. Tang, M. S. Torn, W. D. Collins, G. B. Bonan, D.
834 M. Lawrence, and S. C. Swenson (2013), The effect of vertically resolved soil

biogeochemistry and alternate soil C and N models on C dynamics of CLM4, *Biogeosciences*, *10*, 7109-7131.

Kuzyakov, Y., and X. Xu (2013), Competition between roots and microorganisms for nitrogen: mechanisms and ecological relevance, *New Phytologist*, *198*(3), 656-669.

Lambers, H., C. Mougel, B. Jaillard, and P. Hinsinger (2009), Plant-microbe-soil interactions in the rhizosphere: an evolutionary perspective, *Plant and Soil*, *321*(1-2), 83-115.

Le Quéré, C., R. J. Andres, T. Boden, T. Conway, R. A. Houghton, J. I. House, G. Marland, G. P. Peters, G. R. van der Werf, and A. Ahlström (2013), The global carbon budget 1959–2011, *Earth System Science Data*, *5*(1), 165-185.

Le Quéré, C., M. R. Raupach, J. G. Canadell, and G. Marland (2009), Trends in the sources and sinks of carbon dioxide, *Nature Geoscience*, *2*(12), 831-836.

LeBauer, D. S., and K. K. Treseder (2008), Nitrogen limitation of net primary productivity in terrestrial ecosystems is globally distributed, *Ecology*, *89*(2), 371-379.

Li, C., J. Aber, F. Stange, K. Butterbach‐Bahl, and H. Papen (2000), A process‐oriented model of N2O and NO emissions from forest soils: 1. Model development, *Journal of Geophysical Research: Atmospheres (1984‐2012)*, *105*(D4), 4369-4384.

Maggi, F., C. Gu, W. J. Riley, G. M. Hornberger, R. T. Venterea, T. Xu, N. Spycher, C. Steefel, N. L. Miller, and C. M. Oldenburg (2008), A mechanistic treatment of the dominant soil nitrogen cycling processes: Model development, testing, and application, *Journal of Geophysical Research: Biogeosciences (2005–2012)*, *113*(G2).

Maggi, F., and W. J. Riley (2009), Transient competitive complexation in biological kinetic isotope fractionation explains nonsteady isotopic effects: Theory and application to denitrification in soils, *Journal of Geophysical Research: Biogeosciences (2005–2012)*, *114*(G4).

Marion, G. M., P. C. Miller, J. Kummerow, and W. C. Oechel (1982), Competition for nitrogen in a tussock tundra ecosystem, *Plant and soil*, *66*(3), 317-327.

Marland, G., T. A. Boden, R. J. Andres, A. L. Brenkert, and C. A. Johnston (2003), Global, regional, and national fossil fuel CO2 emissions, *Trends: A compendium of data on global change*, 34-43.

Matson, P., K. A. Lohse, and S. J. Hall (2002), The globalization of nitrogen deposition: consequences for terrestrial ecosystems, *AMBIO: A Journal of the Human Environment*, *31*(2), 113-119.

Matson, P., W. H. McDowell, A. R. Townsend, and P. M. Vitousek (1999), The globalization of N deposition: ecosystem consequences in tropical environments, *Biogeochemistry*, *46*(1-3), 67-83.

McGroddy, M. E., W. L. Silver, R. C. De Oliveira, W. Z. De Mello, and M. Keller (2008), Retention of phosphorus in highly weathered soils under a lowland Amazonian forest ecosystem, *Journal of Geophysical Research: Biogeosciences (2005–2012)*, *113*(G4).

McGuire, A. D., J. M. Melillo, L. A. Joyce, D. W. Kicklighter, A. L. Grace, B. Moore, and C. J. Vorosmarty (1992), Interactions between carbon and nitrogen dynamics in estimating net primary productivity for potential vegetation in North America, *Global Biogeochemical Cycles*, *6*(2), 101-124.

Medvigy, D., S. C. Wofsy, J. W. Munger, D. Y. Hollinger, and P. R. Moorcroft (2009), Mechanistic scaling of ecosystem function and dynamics in space and time: Ecosystem Demography model version 2, *Journal of Geophysical Research: Biogeosciences (2005–2012)*, *114*(G1).

Min, X., M. Y. Siddiqi, R. D. Guy, A. D. M. Glass, and H. J. Kronzucker (2000), A comparative kinetic analysis of nitrate and ammonium influx in two early‐successional tree species of temperate and boreal forest ecosystems, *Plant, Cell & Environment*, *23*(3), 321-328.

Moorcroft, P. R., G. C. Hurtt, and S. W. Pacala (2001), A method for scaling vegetation dynamics: the ecosystem demography model (ED), *Ecological monographs*, *71*(4), 557-586.

Moorhead, D. L., and R. L. Sinsabaugh (2006), A theoretical model of litter decay and microbial interaction, *Ecological Monographs*, *76*(2), 151-174.

Mooshammer, M., W. Wanek, S. Zechmeister-Boltenstern, and A. Richter (2014), Stoichiometric imbalances between terrestrial decomposer communities and their resources: mechanisms and implications of microbial adaptations to their resources, *Frontiers in microbiology*, *5*.

Murray, R. E., L. L. Parsons, and M. S. Smith (1989), Kinetics of nitrate utilization by mixed populations of denitrifying bacteria, *Applied and Environmental Microbiology*, *55*(3), 717-721.

Nedwell, D. B. (1999), Effect of low temperature on microbial growth: lowered affinity for substrates limits growth at low temperature, *FEMS Microbiology Ecology*, *30*(2), 101-111.

Norby, R. J., J. Ledford, C. D. Reilly, N. E. Miller, and E. G. O'Neill (2004), Fine-root production dominates response of a deciduous forest to atmospheric CO2 enrichment, *Proceedings of the National Academy of Sciences of the United States of America*, *101*(26), 9689-9693.

Norby, R. J., J. M. Warren, C. M. Iversen, B. E. Medlyn, and R. E. McMurtrie (2010), CO2 enhancement of forest productivity constrained by limited nitrogen availability, *Proceedings of the National Academy of Sciences*, *107*(45), 19368-19373.

Nordin, A., P. Högberg, and T. Näsholm (2001), Soil nitrogen form and plant nitrogen uptake along a boreal forest productivity gradient, *Oecologia*, *129*(1), 125-132.

Olander, L. P., and P. M. Vitousek (2004), Biological and geochemical sinks for phosphorus in soil from a wet tropical forest, *Ecosystems*, *7*(4), 404-419.

Olander, L. P., and P. M. Vitousek (2005), Short-term controls over inorganic phosphorus during soil and ecosystem development, *Soil Biology and Biochemistry*, *37*(4), 651-659.

Oren, R., D. S. Ellsworth, K. H. Johnsen, N. Phillips, B. E. Ewers, C. Maier, K. V. R. Schäfer, H. McCarthy, G. Hendrey, and S. G. McNulty (2001), Soil fertility

limits carbon sequestration by forest ecosystems in a CO2-enriched atmosphere, *Nature*, *411*(6836), 469-472.
Pappas, C., S. Fatichi, S. Leuzinger, A. Wolf, and P. Burlando (2013), Sensitivity analysis of a process‐based ecosystem model: Pinpointing parameterization and structural issues, *Journal of Geophysical Research: Biogeosciences*, *118*(2), 505-528.
Parton, W. J., E. A. Holland, S. J. Del Grosso, M. D. Hartman, R. E. Martin, A. R. Mosier, D. S. Ojima, and D. S. Schimel (2001), Generalized model for NO x and N2O emissions from soils, *Journal of Geophysical Research: Atmospheres (1984–2012)*, *106*(D15), 17403-17419.
Parton, W. J., J. W. B. Stewart, and C. V. Cole (1988), Dynamics of C, N, P and S in grassland soils: a model, *Biogeochemistry*, *5*(1), 109-131.
Perakis, S. S., and L. O. Hedin (2002), Nitrogen loss from unpolluted South American forests mainly via dissolved organic compounds, *Nature*, *415*(6870), 416-419.
Phillips, R. P., A. C. Finzi, and E. S. Bernhardt (2011), Enhanced root exudation induces microbial feedbacks to N cycling in a pine forest under long‐term CO2 fumigation, *Ecology Letters*, *14*(2), 187-194.
Potter, C. S., J. T. Randerson, C. B. Field, P. A. Matson, P. M. Vitousek, H. A. Mooney, and S. A. Klooster (1993), Terrestrial ecosystem production: a process model based on global satellite and surface data, *Global Biogeochemical Cycles*, *7*(4), 811-841.
Provides, G. F. W. I. (2014), Climate Model Intercomparisons: Preparing for the Next Phase, *Eos*, *95*(9).
Raynaud, X., J.-C. Lata, and P. W. Leadley (2006), Soil microbial loop and nutrient uptake by plants: a test using a coupled C: N model of plant–microbial interactions, *Plant and Soil*, *287*(1-2), 95-116.
Raynaud, X., and P. W. Leadley (2004), Soil characteristics play a key role in modeling nutrient competition in plant communities, *Ecology*, *85*(8), 2200-2214.
Reich, P. B., and S. E. Hobbie (2013), Decade-long soil nitrogen constraint on the CO2 fertilization of plant biomass, *Nature Climate Change*, *3*(3), 278-282.
Reich, P. B., S. E. Hobbie, T. Lee, D. S. Ellsworth, J. B. West, D. Tilman, J. M. H. Knops, S. Naeem, and J. Trost (2006), Nitrogen limitation constrains sustainability of ecosystem response to CO2, *Nature*, *440*(7086), 922-925.
Reynolds, H. L., and S. W. Pacala (1993), An analytical treatment of root-to-shoot ratio and plant competition for soil nutrient and light, *American Naturalist*, 51-70.
Ricciuto, D. M., K. J. Davis, and K. Keller (2008), A Bayesian calibration of a simple carbon cycle model: The role of observations in estimating and reducing uncertainty, *Global biogeochemical cycles*, *22*(2).
Rillig, M. C., M. F. Allen, J. N. Klironomos, N. R. Chiariello, and C. B. Field (1998), Plant species-specific changes in root-inhabiting fungi in a California annual grassland: responses to elevated CO2 and nutrients, *Oecologia*, *113*(2), 252-259.

969 Running, S. W., and J. C. Coughlan (1988), A general model of forest ecosystem
970 processes for regional applications I. Hydrologic balance, canopy gas
971 exchange and primary production processes, *Ecological modelling*, *42*(2),
972 125-154.
973 Schimel, J. P., and J. Bennett (2004), Nitrogen mineralization: challenges of a
974 changing paradigm, *Ecology*, *85*(3), 591-602.
975 Schimel, J. P., L. E. Jackson, and M. K. Firestone (1989), Spatial and temporal effects
976 on plant-microbial competition for inorganic nitrogen in a California annual
977 grassland, *Soil Biology and Biochemistry*, *21*(8), 1059-1066.
978 Scholze, M., T. Kaminski, P. Rayner, W. Knorr, and R. Giering (2007), Propagating
979 uncertainty through prognostic carbon cycle data assimilation system
980 simulations, *Journal of Geophysical Research: Atmospheres (1984–2012)*,
981 *112*(D17).
982 Shen, J., L. Yuan, J. Zhang, H. Li, Z. Bai, X. Chen, W. Zhang, and F. Zhang (2011),
983 Phosphorus dynamics: from soil to plant, *Plant physiology*, *156*(3), 997-1005.
984 Silver, W. L., A. W. Thompson, M. E. McGroddy, R. K. Varner, J. R. Robertson, H. S. J.D.
985 Dias, P. Crill, and M. Keller (2012), LBA-ECO TG-07 Long-Term Soil Gas Flux
986 and Root Mortality, Tapajos National Forest. Data set. Available on-line
987 [http://daac.ornl.gov] from Oak Ridge National Laboratory Distributed
988 Active Archive Center, *Oak Ridge, Tennessee, U.S.A.*,
989 http://dx.doi.org/10.3334/ORNLDAAC/1116.
990 Sokolov, A. P., D. W. Kicklighter, J. M. Melillo, B. S. Felzer, C. A. Schlosser, and T. W.
991 Cronin (2008), Consequences of considering carbon-nitrogen interactions on
992 the feedbacks between climate and the terrestrial carbon cycle, *Journal of*
993 *Climate*, *21*(15), 3776-3796.
994 Springate, D. A., and P. X. Kover (2014), Plant responses to elevated temperatures: a
995 field study on phenological sensitivity and fitness responses to simulated
996 climate warming, *Global change biology*, *20*(2), 456-465.
997 Stocker, T. F., D. Qin, G.-K. Plattner, M. Tignor, S. K. Allen, J. Boschung, A. Nauels, Y.
998 Xia, V. Bex, and P. M. Midgley (2013), Climate Change 2013. The Physical
999 Science Basis. Working Group I Contribution to the Fifth Assessment Report
1000 of the Intergovernmental Panel on Climate Change-Abstract for decision-
1001 makers*Rep.*, Groupe d'experts intergouvernemental sur l'evolution du
1002 climat/Intergovernmental Panel on Climate Change-IPCC, C/O World
1003 Meteorological Organization, 7bis Avenue de la Paix, CP 2300 CH-1211
1004 Geneva 2 (Switzerland).
1005 Tang, J. Y., and W. J. Riley (2013), A total quasi-steady-state formulation of substrate
1006 uptake kinetics in complex networks and an example application to microbial
1007 litter decomposition, *Biogeosciences*, *10*(12), 8329-8351, doi:10.5194/bg-10-
1008 8329-2013.
1009 Tang, J. Y., and W. J. Riley (2014), Weaker soil carbon-climate feedbacks resulting
1010 from microbial and abiotic interactions, *Nature Clim. Change*, *advance online*
1011 *publication*, doi:10.1038/nclimate2438
1012 http://www.nature.com/nclimate/journal/vaop/ncurrent/abs/nclimate2438.html
1013 - supplementary-information.

1014 Templer, P. H., W. L. Silver, J. Pett-Ridge, K. M. DeAngelis, and M. K. Firestone (2008),
1015 Plant and microbial controls on nitrogen retention and loss in a humid
1016 tropical forest, *Ecology*, *89*(11), 3030-3040.
1017 Thomas, R. Q., G. B. Bonan, and C. L. Goodale (2013a), Insights into mechanisms
1018 governing forest carbon response to nitrogen deposition: a model-data
1019 comparison using observed responses to nitrogen addition, *Biogeosciences*
1020 *Discussions*, *10*(1), 1635-1683.
1021 Thomas, R. Q., S. Zaehle, P. H. Templer, and C. L. Goodale (2013b), Global patterns of
1022 nitrogen limitation: confronting two global biogeochemical models with
1023 observations, *Global change biology*, *19*(10), 2986-2998.
1024 Thornton, P. E., J. F. Lamarque, N. A. Rosenbloom, and N. M. Mahowald (2007),
1025 Influence of carbon‐nitrogen cycle coupling on land model response to CO2
1026 fertilization and climate variability, *Global Biogeochemical Cycles*, *21*(4).
1027 Treseder, K. K., and P. M. Vitousek (2001), Effects of soil nutrient availability on
1028 investment in acquisition of N and P in Hawaiian rain forests, *Ecology*, *82*(4),
1029 946-954.
1030 Trumbore, S., E. S. Da Costa, D. C. Nepstad, P. Barbosa De Camargo, L. A. Martinelli, D.
1031 Ray, T. Restom, and W. Silver (2006), Dynamics of fine root carbon in
1032 Amazonian tropical ecosystems and the contribution of roots to soil
1033 respiration, *Global Change Biology*, *12*(2), 217-229.
1034 Vitousek, P. M., and H. Farrington (1997), Nutrient limitation and soil development:
1035 experimental test of a biogeochemical theory, *Biogeochemistry*, *37*(1), 63-75.
1036 Vitousek, P. M., and R. W. Howarth (1991), Nitrogen limitation on land and in the
1037 sea: how can it occur?, *Biogeochemistry*, *13*(2), 87-115.
1038 Vitousek, P. M., S. Porder, B. Z. Houlton, and O. A. Chadwick (2010), Terrestrial
1039 phosphorus limitation: mechanisms, implications, and nitrogen-phosphorus
1040 interactions, *Ecological applications*, *20*(1), 5-15.
1041 Vitousek, P. M., and R. L. Sanford (1986), Nutrient cycling in moist tropical forest,
1042 *Annual review of Ecology and Systematics*, 137-167.
1043 Waksman, S. A. (1931), Principles of soil microbiology, *Principles of soil*
1044 *microbiology.*
1045 Walker, T. W., and J. K. Syers (1976), The fate of phosphorus during pedogenesis,
1046 *Geoderma*, *15*(1), 1-19.
1047 Wang, J., and B. Lars, R (1997), Competition for nitrogen during mineralization of
1048 plant residues in soil: microbial response to C and N availability, *Soil Biology*
1049 *and Biochemistry*, *29*(2), 163-170.
1050 Wang, Y. P., B. Z. Houlton, and C. B. Field (2007), A model of biogeochemical cycles of
1051 carbon, nitrogen, and phosphorus including symbiotic nitrogen fixation and
1052 phosphatase production, *Global Biogeochemical Cycles*, *21*(1).
1053 Wang, Y. P., R. M. Law, and B. Pak (2010), A global model of carbon, nitrogen and
1054 phosphorus cycles for the terrestrial biosphere, *Biogeosciences*, *7*(7), 2261-
1055 2282.
1056 Wieder, W. R., C. C. Cleveland, and A. R. Townsend (2009), Controls over leaf litter
1057 decomposition in wet tropical forests, *Ecology*, *90*(12), 3333-3341.

Woodmansee, R. G., I. Vallis, and J. J. Mott (1981), Grassland nitrogen, *Ecological Bulletins (Sweden)*.

Xu, X., P. E. Thornton, and W. M. Post (2013), A global analysis of soil microbial biomass carbon, nitrogen and phosphorus in terrestrial ecosystems, *Global Ecology and Biogeography*, *22*(6), 737-749.

Yang, X., P. E. Thornton, D. M. Ricciuto, and W. M. Post (2014), The role of phosphorus dynamics in tropical forests–a modeling study using CLM-CNP, *Biogeosciences*, *11*(6), 1667-1681.

Zaehle, S., and D. Dalmonech (2011), Carbon–nitrogen interactions on land at global scales: current understanding in modelling climate biosphere feedbacks, *Current Opinion in Environmental Sustainability*, *3*(5), 311-320.

Zaehle, S., P. Friedlingstein, and A. D. Friend (2010), Terrestrial nitrogen feedbacks may accelerate future climate change, *Geophysical Research Letters*, *37*(1).

Zaehle, S., and A. D. Friend (2010), Carbon and nitrogen cycle dynamics in the O‐CN land surface model: 1. Model description, site‐scale evaluation, and sensitivity to parameter estimates, *Global Biogeochemical Cycles*, *24*(1).

Zaehle, S., B. E. Medlyn, M. G. De Kauwe, A. P. Walker, M. C. Dietze, T. Hickler, Y. Luo, Y. P. Wang, B. El‐Masri, and P. Thornton (2014), Evaluation of 11 terrestrial carbon‐nitrogen cycle models against observations from two temperate Free‐Air CO2 Enrichment studies, *New Phytologist*, *202*(3), 803-822.

Zhang, Q., Y. P. Wang, A. J. Pitman, and Y. J. Dai (2011), Limitations of nitrogen and phosphorous on the terrestrial carbon uptake in the 20th century, *Geophysical Research Letters*, *38*(22).

Zhu, Q., and W. J. Riley (2015), Improved modelling of soil nitrogen losses, *Nature Climate Change*, *5*(8), 705-706.

Zhu, Q., and Q. Zhuang (2013), Modeling the effects of organic nitrogen uptake by plants on the carbon cycling of boreal ecosystems, *Biogeosciences*, *10*(8), 13455-13490.

Zhu, Q., and Q. Zhuang (2014), Parameterization and sensitivity analysis of a process‐based terrestrial ecosystem model using adjoint method, *Journal of Advances in Modeling Earth Systems*.

Appendix A. CNP fluxes

The fluxes of carbon, nitrogen, and phosphorus coming from the upstream pool (i) to the downstream pool (j) due to SOM decomposition are calculated as:

$$F_{C,ij}^{move} = f_{ij} F_{C,i}^{dec} g_i \tag{A1}$$

$$F_{N,ij}^{move} = f_{ij} F_{C,i}^{dec} \min(\frac{1}{CN_i}, \frac{g_i}{CN_j}) \tag{A2}$$

$$F_{P,ij}^{move} = f_{ij} F_{C,i}^{dec} \min(\frac{1}{CP_i}, \frac{g_i}{CP_j}) \tag{A3}$$

where g_i is the percentage of carbon remaining in the soil after decomposition of the i^{th} SOM pool (*i.e.*, CUE, with the rest being released as CO_2); f_{ij} is the fraction of SOM leaving the i^{th} pool and entering the j^{th} pool; and $F_{C,i}^{dec}$ is the first order decay of the i^{th} SOM pool. CN and CP are soil C:N and C:P ratios, respectively.

If the upstream-decomposed soil organic nitrogen (phosphorus) is more than enough to sustain the downstream C:N (C:P) ratio, then the excess nitrogen (phosphorus) enters the soil NH_4^+ (PO_x) pool. PO_x represents the sum of PO_4^{3-}, HPO_4^{2-}, and $H_2PO_4^-$ that could be utilized by plants and microorganisms, and adsorbed by mineral surfaces.

$$F_{N,ij}^{mob} = f_{ij} F_{C,i}^{dec} \max(\frac{1}{CN_i} - \frac{g_i}{CN_j}, 0) \tag{A4}$$

$$F_{P,ij}^{mob} = f_{ij} F_{C,i}^{dec} \max(\frac{1}{CP_i} - \frac{g_i}{CP_j}, 0) \tag{A5}$$

where $F_{N,ij}^{mob}$ and $F_{P,ij}^{mob}$ are the nitrogen and phosphorus gross mineralization rates. Eqn. A4 - A5 ensure that gross mineralization is not less than zero. In contrast, if nitrogen (phosphorus) is insufficient, soil microbes immobilize free NH_4^+ and NO_3^- (PO_x):

$$F_{N,ij}^{immob,pot} = f_{ij} F_{C,i}^{dec} \max(\frac{g_i}{CN_j} - \frac{1}{CN_i}, 0) \quad \text{(A6)}$$

$$F_{NH4,ij}^{immob,pot} = F_{N,ij}^{immob,pot} \cdot \frac{[NH4]}{[NH4]+[NO3]} \quad \text{(A7)}$$

$$F_{NO3,ij}^{immob,pot} = F_{N,ij}^{immob,pot} \cdot \frac{[NO3]}{[NH4]+[NO3]} \quad \text{(A8)}$$

$$F_{P,ij}^{immob,pot} = f_{ij} F_{C,i}^{dec} \max(\frac{g_i}{CP_j} - \frac{1}{CP_i}, 0) \quad \text{(A9)}$$

where $F_N^{immob,pot}$, $F_{NH4}^{immob,pot}$, $F_{NO3}^{immob,pot}$, and $F_P^{immob,pot}$ are microbial N, NH_4^+, NO_3^-, and PO_x immobilization rates. [NH4] and [NO3] are the free NH_4^+ and NO_3^- pools, respectively. We assume that microbes have no preference for NH_4^+ or NO_3^- (Eqn. A7-A8). If soil nutrients are limited, a limitation factor will be applied to those potential soil decomposition CNP fluxes (Eqn. A1 – A9) to maintain the soil organic matter CNP stoichiometry.

Besides decomposing microbe nutrient immobilization, other potential nutrient uptakes are:

$$F_{NH4}^{nit,pot} = [NH4] \cdot k_{nit} \cdot r_\theta \cdot r_T \cdot (1 - f^{anox}) \quad \text{(A10)}$$

$$F_{NO3}^{den,pot} = \min(f(decomp), f([NO3])) \cdot f^{anox} \quad \text{(A11)}$$

$$F_P^{surf,pot} = \frac{VMAX_P^{surf} \cdot KM_P^{surf}}{(KM_P^{surf} + [PO_x])^2} \cdot \frac{d[PO_x]}{dt} \cdot \quad \text{(A12)}$$

where $F_{NH4}^{nit,pot}$, $F_{NO3}^{den,pot}$, and $F_P^{surf,pot}$ are potential rates for NH_4^+ nitrification, NO_3^- denitrification, and mineral surface PO_x adsorption. k_{nit} is the maximum fraction of free NH_4^+ pool that could be utilized by nitrifiers. The potential nitrification rate is controlled by soil temperature (r_T), soil moisture (r_θ), and soil oxygen status ($1\text{-}f^{anox}$). The potential

denitrificaiton rate ($F_{NO3}^{den,pot}$) is either constrained by substrate availability (*f(decomp)*) or NO_3^- availability (*f([NO3])*) [*Del Grosso et al.*, 2000], taking into account the soil anaerobic condition (f^{anox}). $F_P^{surf,pot}$ is derived from the Langmuir adsorption model [*Barrow*, 1978], where adsorbed P is equal to $VMAX_P^{surf} \cdot \frac{[PO_x]}{KM_P^{surf} + [PO_x]}$. Taking the time derivative leads to the adsorption rate [*Wang et al.*, 2010].

Soil NH_4^+ content is altered by inputs from deposition (F_{NH4}^{dep}) and biological N_2 fixation (F^{BNF}) [*Cleveland et al.*, 1999]:

$$F^{BNF} = 1.8 \cdot \frac{1 - e^{-0.003 \cdot NPP_{annual}}}{365 \cdot 86400} \tag{A13}$$

where NPP_{annual} is annual net primary production. Controls on biological N_2 fixation are complex and several models have been developed for large-scale land BGC models [*Cleveland et al.*, 1999; *Fisher et al.*, 2010; *Hartwig*, 1998; *Parton et al.*, 1993; *Running et al.*, 1989; *Vitousek and Field*, 1999]. However, the emergent responses predicted across these model structures are inconsistent [*Galloway et al.*, 2004]. Recognizing this important structural uncertainty, we used a simple model where biological N_2 fixation (F^{BNF}) is modeled as a function of annual NPP [*Cleveland et al.*, 1999].

Soil NO_3^- content is modified by external deposition inputs (F_{NO3}^{dep}) and leaching losses (F_{NO3}^{leach}):

$$F_{NO3}^{leach} = \frac{[NO3]}{W} \cdot Q_{dis} \tag{A14}$$

where soil nitrate concentration ([NO3]: gN m^{-2}) divided by soil water content (W: gH_2O m^{-2}) results in the concentration of dissolved nitrate (DIN). The hydrologic discharge (Q_{dis}: gH_2O m^{-2} s^{-1}) applied to DIN (gN gH_2O^{-1}) leads to the leaching loss (gN m^{-2} s^{-1}).

Soil PO_x content is affected by external inputs from parent material weathering ($F^{weather}$) and leaching losses (F_P^{leach}). Sorbed P (P_S) could be further strongly occluded and become unavailable for plant and microbial uptake. Parent material stock can be increased by atmospheric dust deposition (F_P^{dep}) [*Mahowald et al.*, 2008]:

$$F^{weather} = [P_P] \cdot k_{weather} \quad \text{(A15)}$$

$$F_P^{leach} = \frac{[PO_x]}{W} \cdot Q_{dis} \quad \text{(A16)}$$

$$F_P^{occl} = [P_S] \cdot k_{occl} \quad \text{(A17)}$$

where parent material weathering ($F^{weather}$) is calculated using a weather rate ($k_{weather}$) and parent material P content ($[P_P]$). PO_x leaching loss is modeled with a similar approach to nitrate leaching (Eqn. A16). Phosphorus occlusion rate is modeled as the product of a constant rate (k_{occl}) and the sorbed P content ($[P_S]$).

References:

Barrow, N. J. (1978), The description of phosphate adsorption curves, *Journal of Soil Science*, *29*(4), 447-462.

Cleveland, C. C., A. R. Townsend, D. S. Schimel, H. Fisher, R. W. Howarth, L. O. Hedin, S. S. Perakis, E. F. Latty, J. C. Von Fischer, and A. Elseroad (1999), Global patterns of terrestrial biological nitrogen (N2) fixation in natural ecosystems, *Global Biogeochemical Cycles*, *13*(2), 623-645.

Del Grosso, S. J., W. J. Parton, A. R. Mosier, D. S. Ojima, A. E. Kulmala, and S. Phongpan (2000), General model for N2O and N2 gas emissions from soils due to dentrification, *Global Biogeochemical Cycles*, *14*(4), 1045-1060.

Fisher, J. B., S. Sitch, Y. Malhi, R. A. Fisher, C. Huntingford, and S. Y. Tan (2010), Carbon cost of plant nitrogen acquisition: A mechanistic, globally applicable model of plant nitrogen uptake, retranslocation, and fixation, *Global Biogeochemical Cycles*, *24*(1).

Galloway, J. N., F. J. Dentener, D. G. Capone, E. W. Boyer, R. W. Howarth, S. P. Seitzinger, G. P. Asner, C. C. Cleveland, P. A. Green, and E. A. Holland (2004), Nitrogen cycles: past, present, and future, *Biogeochemistry*, *70*(2), 153-226.

Hartwig, U. A. (1998), The regulation of symbiotic N< sub> 2</sub> fixation: a conceptual model of N feedback from the ecosystem to the gene expression level, *Perspectives in Plant Ecology, Evolution and Systematics*, *1*(1), 92-120.

Mahowald, N., T. D. Jickells, A. R. Baker, P. Artaxo, C. R. Benitez-Nelson, G. Bergametti, T. C. Bond, Y. Chen, D. D. Cohen, and B. Herut (2008), Global distribution of atmospheric phosphorus sources, concentrations and deposition rates, and anthropogenic impacts, *Global Biogeochemical Cycles*, *22*(4).

Parton, W. J., J. M. O. Scurlock, D. S. Ojima, T. G. Gilmanov, R. J. Scholes, D. S. Schimel, T. Kirchner, J. C. Menaut, T. Seastedt, and E. Garcia Moya (1993), Observations and modeling of biomass and soil organic matter dynamics for the grassland biome worldwide, *Global biogeochemical cycles*, *7*(4), 785-809.

Running, S. W., R. R. Nemani, D. L. Peterson, L. E. Band, D. F. Potts, L. L. Pierce, and M. A. Spanner (1989), Mapping regional forest evapotranspiration and photosynthesis by coupling satellite data with ecosystem simulation, *Ecology*, 1090-1101.

Vitousek, P. M., and C. B. Field (1999), Ecosystem constraints to symbiotic nitrogen fixers: a simple model and its implications, *Biogeochemistry*, *46*(1-3), 179-202.

Wang, Y. P., R. M. Law, and B. Pak (2010), A global model of carbon, nitrogen and phosphorus cycles for the terrestrial biosphere, *Biogeosciences*, *7*(7), 2261-2282.

Appendix B. Derivation of *VMAX*

The enzyme substrate reaction is: $S + E \underset{k_1^-}{\overset{k_1^+}{\longleftrightarrow}} C \xrightarrow{k} P + E$, where the enzyme ($E$) and substrate ($S$) reaction is reversible and forms complex (C). The irreversible reaction releases product (P) and liberates enzyme (E). At steady state, the formation rate of the enzyme substrate complex is equal to the consumption rate:

$$k_1^+[S][E] = k_1^-[C] + k[C] \tag{B1}$$

To simply the equation, we define an affinity parameter:

$$KM = \frac{k_1^- + k}{k_1^+} = \frac{[S]\cdot[E]}{[C]} \tag{B2}$$

By definition, the total enzymes $[E_{tot}]$ in the system is the sum of free enzymes $[E]$ and enzymes that are bound with the substrate $[C]$:

$$[E_{tot}] = [E] + [C] \tag{B3}$$

Substituting Eqn. (B3) into (B2), we have:

$$KM = \frac{[S]\cdot([E_{tot}] - [C])}{[C]} \tag{B4}$$

Collecting terms containing [C], we have:

$$[C]\cdot(KM + [S]) = [E_{tot}]\cdot[S] \tag{B5}$$

The production rate is:

$$\frac{d[P]}{dt} = k\cdot[C] \tag{B6}$$

Substituting Eqn. (B5) into (B6), we have:

$$\frac{d[P]}{dt} = k\cdot[E_{tot}]\cdot\frac{[S]}{KM + [S]} \tag{B7}$$

Comparing Eqn. (B7) with the classic Michaelis-Menten equation, it is clear that the definition of maximum production rate is the product of the reaction rate and enzyme abundance in the system:

$$VMAX = k \cdot [E_{tot}] \tag{B8}$$

Figure A1. MCMC chain. Blue line represents the MCMC samples that are used to infer our model posterior parameters. Two other replicated MCMC calibrations (with different random number seeds) were conducted (yellow and red lines), in order to check the convergence of MCMC calibration.

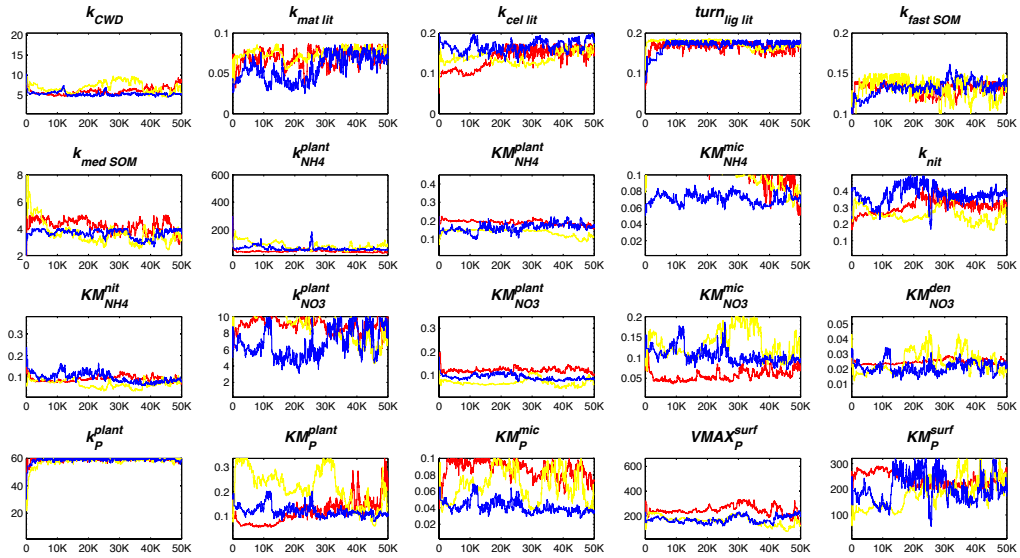

Figure A2. Gelman-Rubin convergence criterion calculated from three chains in Figure A1. Baseline value is commonly set to 1.1 (red line). When the Gelmen-Rubin criterion is less than or equal to 1.1, the multiple chains are thought to converge.

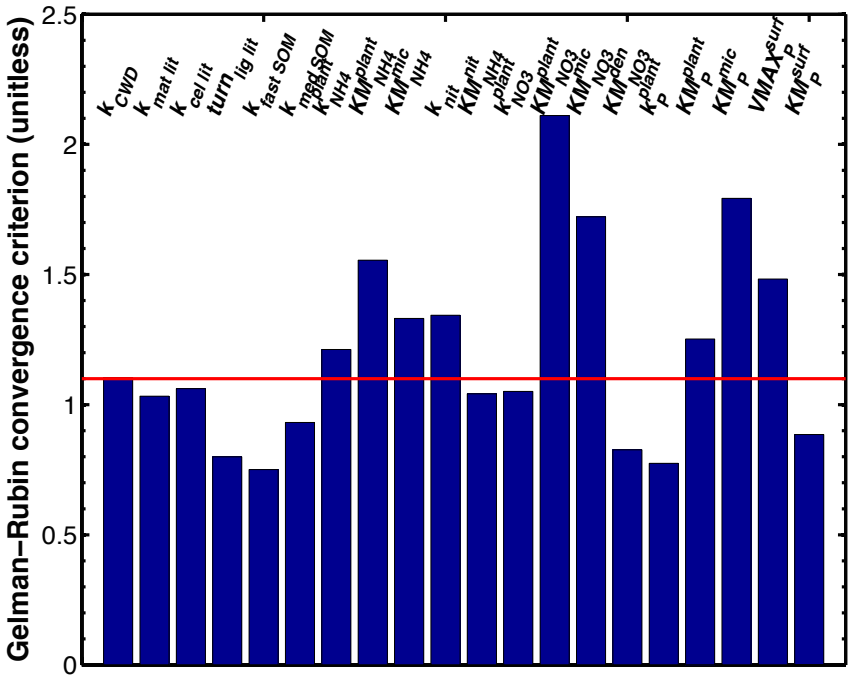

Figure A3. Posterior model parameters (blue bars) fitted to Gaussian distribution (red line).